

STARS


University of Central Florida
STARS

Electronic Theses and Dissertations, 2004-2019

2006

Electrical Properties Of Reactive Magnetron Sputtered Vanadium Oxide Thin Films

Vu Huynh Lam
University of Central Florida

 Part of the [Electrical and Computer Engineering Commons](#)
Find similar works at: <https://stars.library.ucf.edu/etd>
University of Central Florida Libraries <http://library.ucf.edu>

This Masters Thesis (Open Access) is brought to you for free and open access by STARS. It has been accepted for inclusion in Electronic Theses and Dissertations, 2004-2019 by an authorized administrator of STARS. For more information, please contact STARS@ucf.edu.

STARS Citation

Lam, Vu Huynh, "Electrical Properties Of Reactive Magnetron Sputtered Vanadium Oxide Thin Films" (2006). *Electronic Theses and Dissertations, 2004-2019*. 6127.
<https://stars.library.ucf.edu/etd/6127>



ELECTRICAL PROPERTIES OF REACTIVE MAGNETRON SPUTTERED VANADIUM
OXIDE THIN FILMS

by

VU HUYNH LAM
B.S. University of Central Florida, 2005

A thesis submitted in partial fulfillment of the requirements
for the degree of Master of Science
in the School of Electrical Engineering and Computer Science
in the College of Engineering and Computer Science
at the University of Central Florida
Orlando, Florida

Fall Term
2006

© 2006 Vu Huynh Lam

ABSTRACT

It is well known that vanadium oxide can take many different forms. However for this study, only the amorphous phase was investigated. Amorphous vanadium oxide (VO_x) thin films were deposited on thermally grown silicon dioxide by DC magnetron sputtering using a vanadium metal target in an argon / oxygen atmosphere. The driving force of this study was to investigate the temperature coefficient of resistance (TCR) and low resistivity in the amorphous films. Sheet resistance is very sensitive to small changes in temperature, making amorphous VO_x very attractive to thermal sensor applications such as infrared detectors.

To form the vanadium oxide, physical vapor deposition of vanadium metal at 200 Watts of DC power was used with varied amounts of oxygen in a primary argon atmosphere. During deposition, the concentration of oxygen was controlled by using a 20:80 mixture of O_2 and Ar in conjunction with high purity Ar supply. Flow control techniques were derived and calculated to predict the percentage of oxygen before and during deposition to understand the reaction between the vanadium metal and oxygen. Concentrations of O_2 in the deposition chamber were varied from 0.025% to 3.000% with the purpose of gaining an understanding of the affects of O_2 concentration in amorphous VO_x films. TCR and resistivity measurements were performed to characterize the films. The results showed a resistivity decrement with decreasing oxygen concentration. The films with lower concentrations of oxygen were found to have better TCR values then those with higher percentages of oxygen.

To further reduce the resistivity of the VO_x and maintain the TCR value, co-sputtering of noble metals (gold and platinum) with VO_x was studied. The metals were co-sputtered at various power settings with the vanadium oxide reactive process at a fixed percentage of oxygen. The

TCR and resistivity results showed that the additions of Au and Pt into VO_x reduced the resistivity. However, only Au was found to improve TCR value.

The results of these experiments showed that by reducing the amount of oxygen in the film, the ratio between TCR and resistivity further improved. Mechanical limits of the gas delivery system and the relatively low sensitivity to oxygen detection, gas flow control is limited when sputtering with only a single target. Several targets were therefore used during sputtering to allow for higher gas flows thereby increasing the effective sensitivity of the oxygen control. To increase the amount of available vanadium and still have a sufficient amount of detectible oxygen present, four vanadium targets were sputtered simultaneously. The measurements appeared to have a trend of increase in TCR values with a decrease in resistivity. For an ideal case, thermal sensor material should incorporate high TCR and low resistivity for better sensitivity. The amorphous vanadium oxide deposited by 4 vanadium targets seems to satisfy that requirement. In conclusion, a novel method has been established to fabricate amorphous vanadium oxide thin films with high TCR and low resistivity for infrared detectors.

ACKNOWLEDGMENTS

First and foremost, I would like to acknowledge and thank my advisors Dr. Kevin R. Coffey and Dr. Kalpathy B. Sundaram for their guidance and support throughout the years. I would also like to thank to Dr. Jiann S. Yuan for serving on my thesis committee.

I am grateful to Ravi M. Todi for introducing me to the semiconductor material processing and for his valuable guidance. I am also wish to acknowledge Mr. Edward Dein who always inspired and gave helpful suggestions to improve and understand experimental methods and data analysis.

I would like to thank my colleagues Andrew Warren for making the XRD measurements and helping with the understanding of the analysis and Bo Yao for preparing the RBS samples and the analysis of the data. My thanks to Arun Vijayakumar and Matthew Ericson for their help editing my thesis. And at last, I would like to thank my family for their love and moral support at all times.

TABLE OF CONTENTS

LIST OF FIGURES	vii
LIST OF TABLES	ix
LIST OF ACRONYMS/ABBREVIATIONS	x
CHAPTER ONE: INTRODUCTION.....	1
CHAPTER TWO: LITERATURE REVIEW.....	5
CHAPTER THREE: METHODOLOGY	12
3.1 The Reactive Magnetron Sputtering System	12
3.2 The Deposition Process.....	16
3.3 Sample Preparation	18
3.4 Measurements	21
3.5 Improvements	25
CHAPTER FOUR: RESULTS AND DISCUSSION.....	27
4.1 Experiments Summary.....	27
4.2 Single Vanadium Target Depositions	28
4.3 Noble Metals Co-Sputtered With Single Vanadium Target	33
4.4 Four Vanadium Targets Depositions	45
CHAPTER FIVE: CONCLUSION.....	52
LIST OF REFERENCES.....	53

LIST OF FIGURES

Figure 1.1 An Example of an Infrared Image.....	1
Figure 1.2 The Focal Plane Array of an Infrared Detector.....	2
Figure 1.3 Structure of a Microbolometer.....	3
Figure 1.4 A Zoom In Image of a Microbolometer.....	4
Figure 2.1 Variable E_g in Hypothetical Silicon.....	7
Figure 2.2 Hysteretic and Non-hysteretic Property of Crystalline and Amorphous VO_x	9
Figure 2.3 Dual Ion Beam Sputtered VO_x from Zintu, et. al.. [24].....	10
Figure 3.1 Single Vanadium Target Sputtered in Different Percentages of O_2	13
Figure 3.2 (a) Metallic Phase (b) Fully Oxidized Phase.....	14
Figure 3.3 Reactive Magnetron Sputtering System.....	15
Figure 3.4 Reaction Between Oxygen and Vanadium.....	17
Figure 3.5 Sample Preparations for Thickness Measurement.....	18
Figure 3.6 Sample Preparations for Sheet Resistance Measurement.....	19
Figure 3.7 Sample Preparations for TCR Measurement.....	20
Figure 3.8 Thickness Measurement Technique.....	21
Figure 3.9 Sheet Resistance Measurement Technique.....	22
Figure 3.10 Temperature Coefficient of Resistance Measurement System.....	24
Figure 4.1 Resistivity vs. Percentages of O_2 in Single Vanadium Target Depositions.....	29
Figure 4.2 TCR vs. Percentages of O_2 in Single Vanadium Target Depositions.....	30
Figure 4.3 TCR vs. Resistivity in Single Vanadium Target Depositions.....	31
Figure 4.4 Metal Additions to Amorphous VO_x Thin Film.....	32

Figure 4.5 Resistivity vs. DC Power of Pt Additions VO _x Thin Films.	34
Figure 4.6 TCR vs. DC Power of Pt Additions VO _x Thin Films.	34
Figure 4.7 TCR vs. Resistivity of Pt Additions VO _x Thin Films.	35
Figure 4.8 Resistivity vs. DC Power of Au Additions VO _x Thin Films.	36
Figure 4.9 TCR vs. DC Power of Au Additions VO _x Thin Films.	37
Figure 4.10 TCR vs. Resistivity of Au Additions VO _x Thin Films.	37
Figure 4.11 TCR vs. Resistivity of Pt and Au Addition VO _x with Respect to Zintu, et. al.	38
Figure 4.12 Resistivity vs. DC Power of 2 nd Au Additions VO _x Thin Films.	40
Figure 4.13 TCR vs. DC Power of 2 nd Au Additions VO _x Thin Films.	40
Figure 4.14 TCR vs. Resistivity of 1 st and 2 nd Au Additions VO _x Thin Films.	41
Figure 4.15 TCR vs. Resistivity of 1 st and 2 nd Au Additions VO _x with Respect to Zintu, et. al.	42
Figure 4.16 Reaction Rates of Oxygen and Vanadium for Single Target and Four Targets.	46
Figure 4.17 4 Vanadium Targets Deposition with and without Liquid Nitrogen Cryo-Pump.	47
Figure 4.18 Resistivity vs. Percentages of O ₂ for 4 Vanadium Targets Depositions.	48
Figure 4.19 TCR vs. Percentages of O ₂ in 4 Vanadium Targets Depositions.	49
Figure 4.20 TCR vs. Resistivity in 4 Vanadium Targets Depositions.	50
Figure 4.21 TCR vs. Resistivity in 4 Vanadium Targets Depositions with Respect to Zintu, et. al.	50

LIST OF TABLES

Table 4.1 Single Vanadium Target Deposition Data.....	28
Table 4.2 Noble Metals Co-Sputter Single Vanadium Target Depositions.....	43
Table 4.3 Four Vanadium Targets Depositions.....	51

LIST OF ACRONYMS/ABBREVIATIONS

Ar / O ₂	Argon / Oxygen Gas Mixture
Ar	Argon Gas
Au	Gold
C	Degree in Celsius
CMOS	Complementary Metal Oxide Semiconductor
DC	Direct Current
E _g	Activation Energy
IR	Infrared
O ₂	Oxygen
PC	Personal Computer
Pt	Platinum
RF	Radio Frequency
RGA	Residual Gas Analysis
ROIC	Read Out Integrated Circuit
R _s	Sheet Resistance
SCCM	Standard Cubic Centimeter per Minute
T	Temperature
TCR	Temperature Coefficient Resistance
V	Vanadium
VO _x	Vanadium Oxide

CHAPTER ONE: INTRODUCTION

Infrared imaging technology has changed greatly due to the development of micromachining technology. Traditionally, infrared sensor has to perform in cryogenic environment to ensure high performance. However with micromachining technology, infrared sensor can operate at room temperature and still maintaining good performance. Figure 1.1 below illustrated an example of an infrared image [10]. The focal plane array of the infrared sensor is an array of microbolometers in which used to absorb infrared radiation as Figure 1.2 illustrated [10].



Figure 1.1 An Example of an Infrared Image.

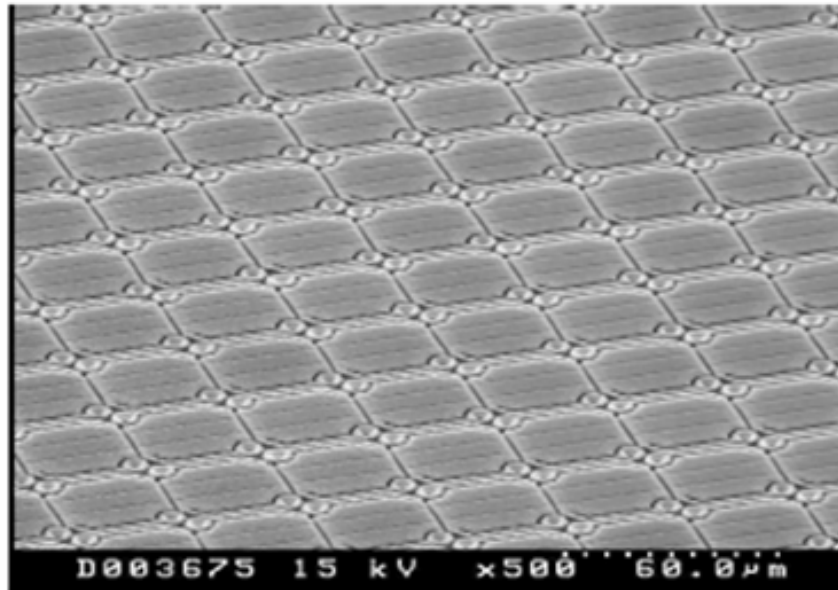


Figure 1.2 The Focal Plane Array of an Infrared Detector.

Each microbolometer has a thermal sensitive layer that changes its sheet resistance with temperature. The basic operation of a bolometer can be described as follows. Infrared radiation emitted and absorbed through a bolometer that changes the resistance of the bolometer thin film. This change in resistance will be obtained and converted into an image by the CMOS Read out Integrated Circuit (ROIC) below. A microbolometer has a micro-bridge structure that is uniquely designed for infrared detection as shown in Figures 1.3 and 1.4 [10]. The bridge structure prevents heat from escaping through the CMOS ROIC and maintains good sensitivity of the bolometer. The diaphragm is suspended above the integrated circuit to maintain good thermal isolation. The cavity beneath the diaphragm is designed to have a distance of $\frac{1}{4} \lambda$ to improve infrared absorption. Also, the beam supporting the diaphragm is designed to have an appropriate distance in order to optimize heat transportation. If the arm is too long, the heat obtained will slowly disperse, which causes poor imaging when the next infrared radiation arrives. If the arm is too short, the heat will

quickly escape and device sensitivity will be decreased. An ideal bolometer material would have high temperature coefficient of resistance (TCR) and low resistivity to maintain high sensitivity. Vanadium oxide has been established and well recognized to be a material that have high resistivity change with temperature and is suitable for bolometer fabrication.

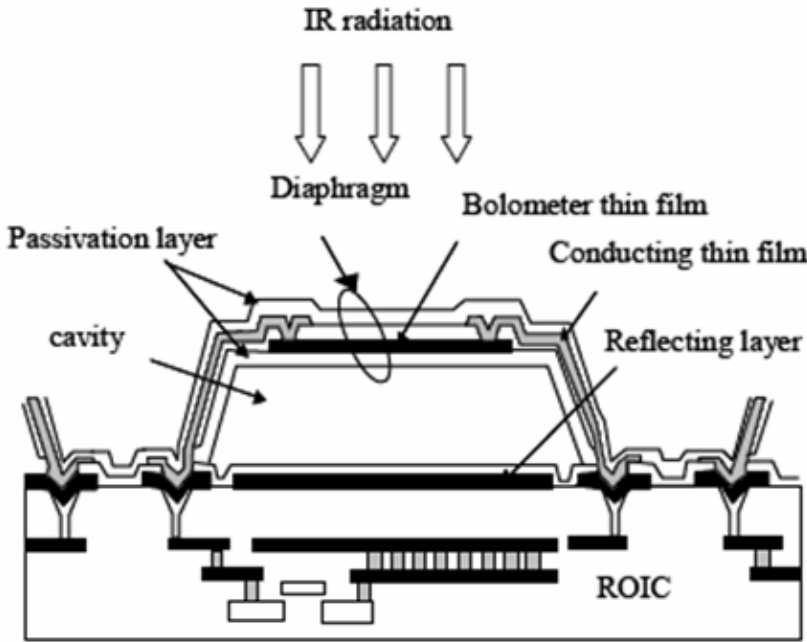


Figure 1.3 Structure of a Microbolometer.

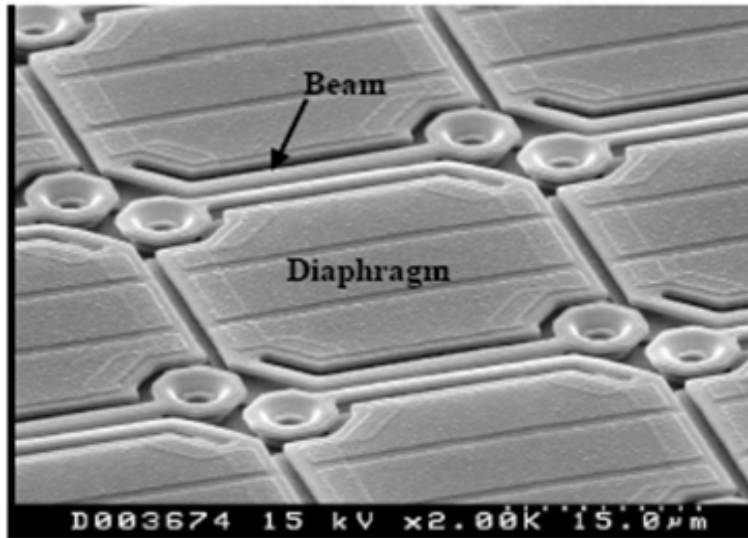


Figure 1.4 A Zoom In Image of a Microbolometer.

For this study, vanadium oxide thin films have been deposited using DC magnetron sputtering method and the electrical properties were characterized such as TCR and resistivity. The results of the deposited vanadium oxide displayed a high TCR values with low resistivity. However, in order to improve the sensitivity of the bolometer thin film, resistivity of vanadium oxide films can be further reduced. For this purpose, noble metals such as platinum and gold are used to co-sputter with vanadium to deposited vanadium oxide. Platinum doped vanadium oxide yields a great reduction in resistivity, however, its TCR values also reduced as well. Unlike platinum, gold doped vanadium oxide presents a smaller reduction in resistivity but maintains high TCR values. An alternative method to reduce resistivity of vanadium oxide is by lowering the percentage of oxygen concentration while using four vanadium metals. The results presented a new relationship between the TCR and resistivity values which makes it a novel method to develop an ideal material for bolometer thin film.

CHAPTER TWO: LITERATURE REVIEW

Vanadium oxide is a semiconductor material that is well established for infrared sensors. Vanadium oxide is a preferred material over other semiconductors due to its high temperature coefficient of resistance (TCR) with respect to its resistivity values. It obtains high TCR with small resistivity. Both TCR and resistivity are two important parameters that determine the performance of the bolometer thin films used in infrared imaging. Unfortunately, the TCR of semiconductors has a simple physical limit which determines their performance for bolometer thin film. In general, a higher TCR values is accompanied by an extremely high resistivity. For example, intrinsic silicon can be used to demonstrate the TCR and resistivity relationship with respect to band gap energy. The resistivity of intrinsic silicon at room temperature can be written as follows:

$$\rho = \frac{m}{ne^2\tau} \propto e^{\frac{E_g}{kT}} \quad (2.1)$$

where m is the effective mass, n is the thermally activated intrinsic carrier concentration of silicon, e is the electron charge, τ is the mean free time, E_g is the band gap energy, k is Boltzmann constant, and T is the temperature. With this equation, resistivity can be viewed as a function of band gap energy. This approach can be also applied to calculate the TCR values of intrinsic silicon,

$$\alpha = \frac{1}{R} \frac{dR}{dT} \quad (2.2)$$

where α is the TCR value, and R is the resistance of the film. R can also be expressed as follows,

$$R = R_o e^{\frac{E_g}{kT}} \quad (2.3)$$

where R_o is the resistance at room temperature. The TCR equation can be further simplified as follows,

$$\alpha \approx \frac{-E_g}{kT} \frac{1}{T} \propto \frac{E_g}{T^2} \quad (2.4)$$

Figure 2.1 illustrates TCR and resistivity values of hypothetical intrinsic silicon at room temperature having a range of different band gap energies. This shows that semiconductors can have very high TCR values; however, their resistivity will be very high as well. Bolometer thin film are required to have high TCR in order to maintain high sensitivity with and low resistivity for compatibility with low noise readout for infrared imaging devices. From this figure, it can be seen that large band gap semiconductors can be used as a sensor materials with high TCR values, but the high resistivity will not be compatible with readout electronics. Amorphous vanadium oxide is a preferred semiconductor material for infrared imaging bolometer thin film applications due to it relatively high TCR at modest resistivity, and because it can be processed at the relatively low temperatures ($< 200^\circ\text{C}$) required for integration in imaging systems.

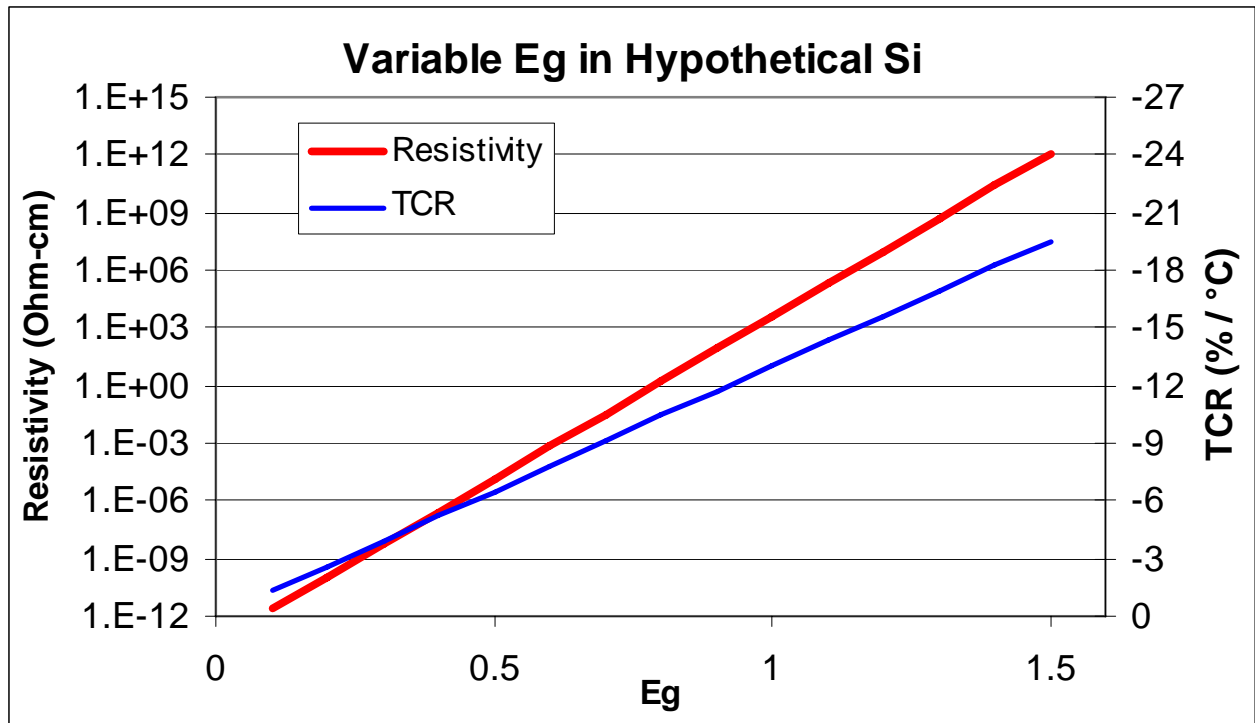


Figure 2.1 Variable E_g in Hypothetical Silicon.

Vanadium oxides can have multiple stoichiometries and can be categorized based on their structures as crystalline or amorphous. Research has been performed to study these properties of both types of structures. Crystalline vanadium oxide has shown a dramatic resistivity vs. temperature effects due to a semiconductor to metal phase transition. When the temperature rises over a transition point, the crystal structure of VO_2 will change from a monoclinic phase into tetragonal rutile phase. At the same time, high optical transmission of the crystalline vanadium oxide will change to low optical transmission [12]. Different compositions of crystalline vanadium oxides experience phase transitions at different temperatures. For example, when the temperature reaches $68^\circ C$, VO_2 undergoes a phase transition. V_2O_3 has a different crystal

structure and also undergoes a phase transition, at the much lower temperature of -134°C . V_2O_5 has yet another structure and changes to metallic state at higher temperature, 250°C [19].

For crystalline VO_2 , the resistance can drop 5 orders of magnitude at the transition temperature, which makes it very attractive to many applications such as photoelectric switch, solar control, and defense laser radiation [28]. Unfortunately, this phase transition is hysteretic. Figure 2.2 illustrates the hysteretic property of crystalline (annealed) VO_2 as compared to the amorphous VO_x (un-annealed) [32]. For example, VO_2 undergoes a phase transition at 68°C . Its resistance will decrease. However, when the resistance is at the mid point of the transition, a temperature change has no effect on its resistance. The imaging performance of a bolometer thin film will suffer greatly due to this property. Unlike crystalline VO_2 , the amorphous VO_x does not incorporate this property as figure 2.2 illustrates. Its resistance changes according to the change of temperature in a linear fashion. When the temperature is heating up or cooling down, the resistance will change its value accordingly.

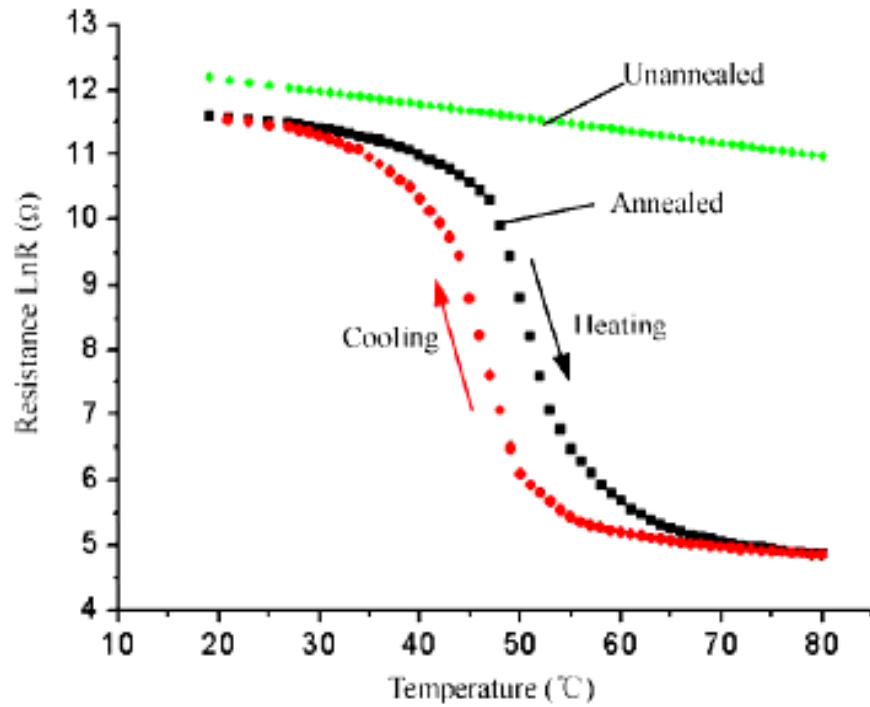


Figure 2.2 Hysteretic and Non-hysteretic Property of Crystalline and Amorphous VO_x .

Therefore, amorphous VO_x is a better choice for sensor applications for its non-hysteretic property. Many applications have used amorphous VO_x as a sensor material due to its high TCR value and low resistivity. Such applications include light detectors, surveillance, night vision, detection of gas leakage, infrared detectors, and thermochromic smart windows [1-11].

Many other amorphous semiconductors have been studied as alternative films for bolometer applications. Such materials include amorphous silicon, yttrium barium copper oxide (YBCO), and amorphous germanium [24]. So far, amorphous vanadium oxide seems to be the preferred material for bolometer applications.

Figure 2.3 illustrates the relationship between TCR and resistivity values of amorphous VO_x formed by the dual ion beam sputtering technique [24]. This relationship also shows the trend of increasing TCR with increasing resistivity expected of semiconductors.

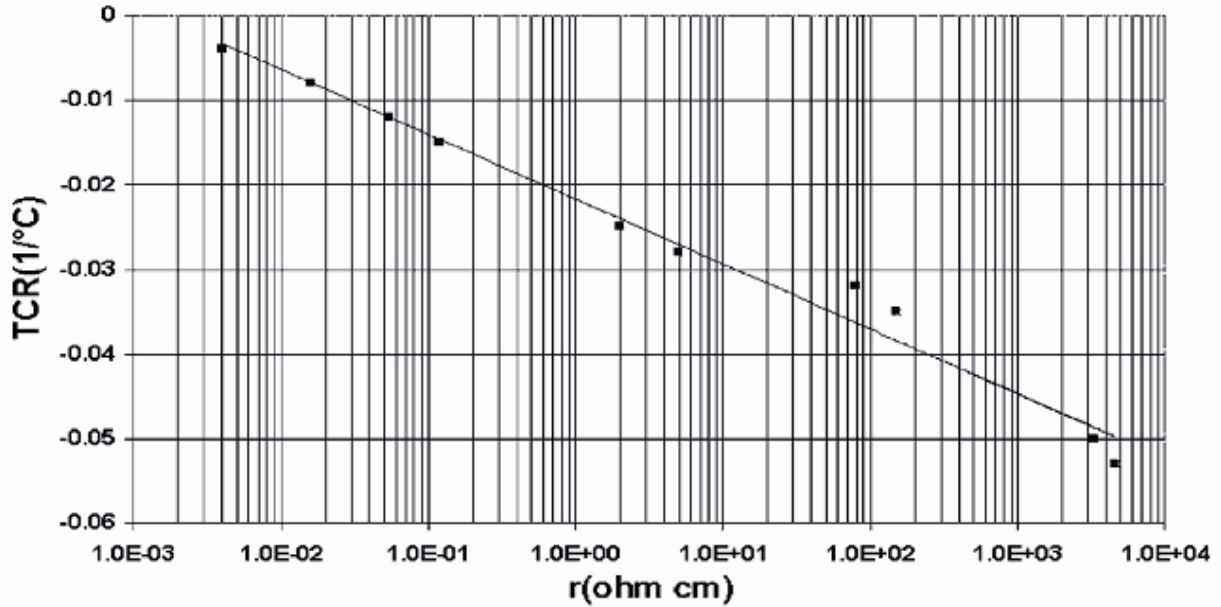


Figure 2.3 Dual Ion Beam Sputtered VO_x from Zintu, et. al.. [24]

We can use this figure as a reference to determine the goals of our efforts to develop vanadium oxide. An improved vanadium oxide will have a higher TCR and/or lower resistivity than that shown in figure 2.3 and poorly performing vanadium oxide will have a lower TCR and/or higher resistivity. A variety of deposition techniques have been used to develop vanadium oxides, however, the majority of outcomes tend to be crystalline vanadium oxide. Such techniques include thermal evaporation [23], ion beam deposition [22-24], pulse laser deposition [25], [26], atomic layer chemical vapour deposition [27], and reactive magnetron sputtering

deposition [12-18]. The most common and simplified technique to develop vanadium oxide is reactive magnetron sputtering deposition. With this technique, crystalline and amorphous vanadium oxide can be formed.

Other parameters that are used to control the crystal structure of vanadium oxide are the temperature and the oxygen concentration during and after deposition. The most common technique found in literature is to anneal the deposited vanadium oxide sample in oxygen / argon ambient at high or low temperature to yield a crystalline film. Studies have performed to develop vanadium oxide with different range of temperatures and different percentages of oxygen concentration to yield variety of vanadium oxide compositions. These compositions can be either crystalline or amorphous [28-43]. The compositions of the crystalline materials are VO_2 , V_2O_3 , and V_2O_5 . Elevated temperature, in the range of 200°C to 500°C , can use during deposition or during post-deposition annealing to promote crystallization of the vanadium oxide sample. The percentages of oxygen can range from 6% to 50%. Within these ranges of temperature and oxygen, the resulting vanadium oxide is typically crystalline. Our study is focused on amorphous vanadium oxide thin films, therefore, room temperature deposition in a low percentage of oxygen is used and no post-deposition annealing is performed.

CHAPTER THREE: METHODOLOGY

3.1 The Reactive Magnetron Sputtering System

Amorphous vanadium oxide was chosen as the primary material to study for this project. Sputtering processes normally uses argon gas because it does not react with the target material allowing thin films to be formed. The addition of a gas that reacts with the target material, such as oxygen, will form compounds of the material and the reactant. To determine how vanadium oxide is formed using reactive magnetron sputtering a reactive gas test was performed.

Because the sputtering system uses a DC power supply that allows both voltage and current to float while maintaining constant power, the target voltage can be easily measured and used to infer changes in the impedance of the sputtering plasma. The gun in which the target is mounted is designed to provide a narrow range of impedance to the power supply. With the addition of a reactive gas the impedance of the target changes. Using the fixed conditions of 200 Watts of DC power and a chamber pressure of 4.0 mTorr while introducing increased amounts of oxygen the voltages were recorded. Figure 3.1 illustrated the outcome of this experiment.

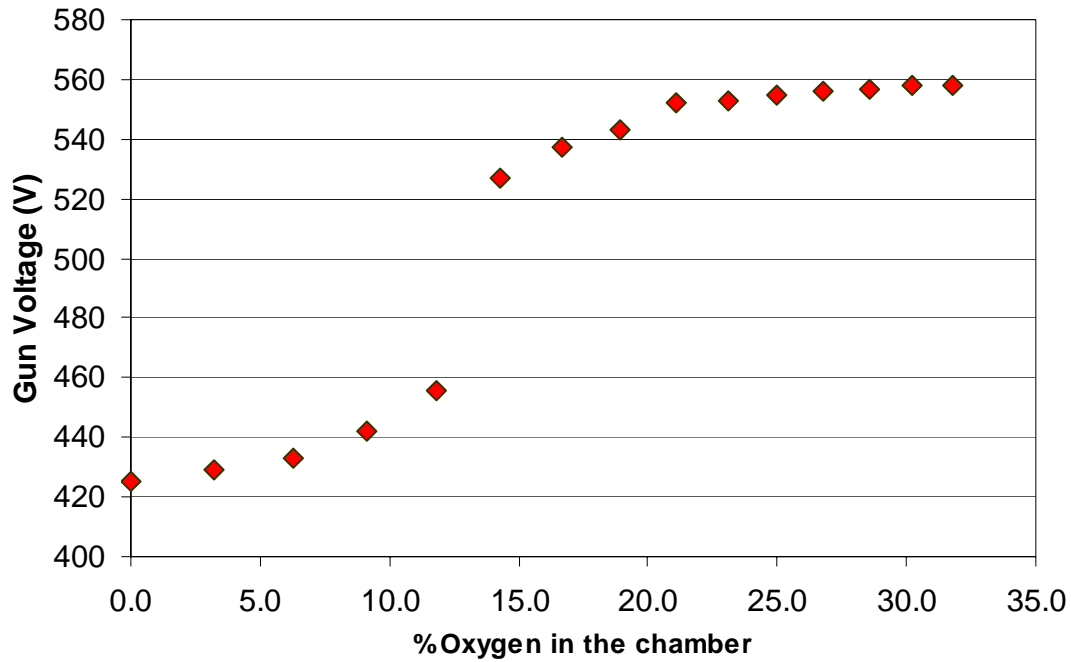


Figure 3.1 Single Vanadium Target Sputtered in Different Percentages of O₂.

The plot of gun voltage vs. oxygen percentage has two distinct regions and a very sharp transition point. The lower voltage region, less than about 12.5% oxygen, corresponds to primary metallic vanadium target surface while for oxygen concentrations above 15% the target surface is fully oxidized.

In the metallic region, both argon and oxygen ions bombarded the target's surface to sputter away metallic vanadium atoms and those that have reacted with oxygen. With small amount of oxygen concentration in the chamber both vanadium and vanadium oxide can be sputtered from the target surface as figure 3.2a illustrates. As these atoms condense on the substrate surface, further oxidation can occur to form an amorphous VO_x thin film. As the oxygen concentration in the deposition chamber increases, the target surface begins to oxidize

and will continue to oxidize until the entire surface is fully oxidized. At this point only vanadium oxide is sputtered from the target surface as illustrated in figure 3.2b. This effect is known as target poisoning because the deposition rate is severely reduced. For our application we must maintain low resistivity and high TCR values, thus the low oxygen concentration, metallic region is preferred.

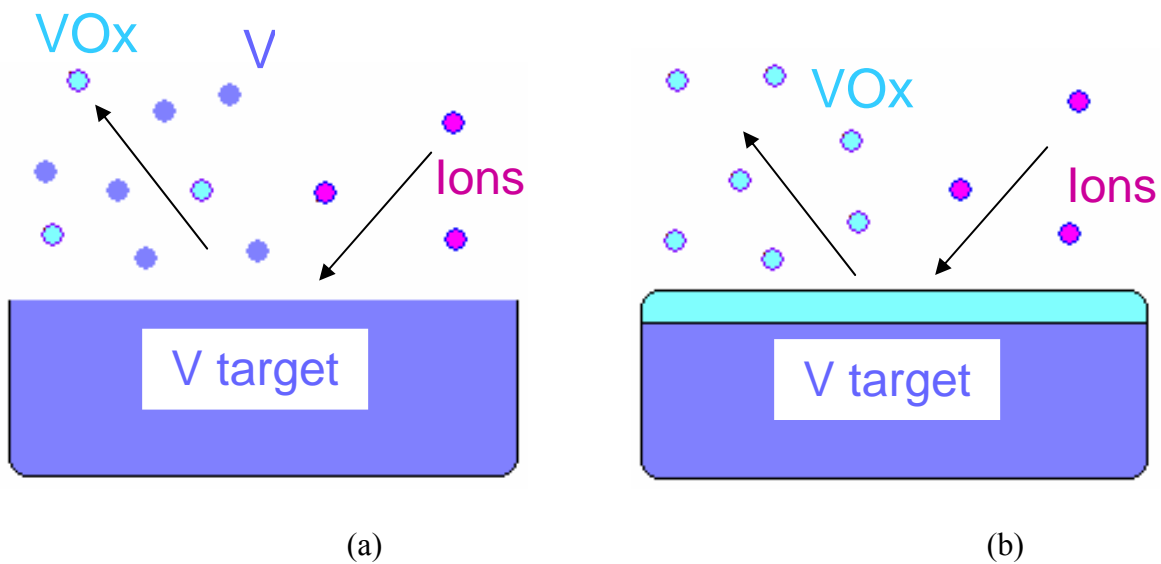


Figure 3.2 (a) Metallic Phase (b) Fully Oxidized Phase.

Figure 3.3 illustrates the basic schematic of the sputtering system used to produce the thin film samples. The sputter system has two chambers, a load lock chamber and the main process chamber. The load lock chamber is used to isolate the process chamber from exposure to the atmosphere. A magnetically coupled load arm is used to deliver/remove samples to/from the main chamber. The main chamber has six sputter guns that are individually driven by four DC and 2 RF power supplies. The process pressure is maintained by a closed loop control system

consisting of a variable gate valve and a capacitance monometer pressure sensor. Process gases are controlled by mass flow controllers and are independent of the chamber pressure controller. A residual gas analyzer (RGA) is used to measure the partial pressure of all the gases present inside the chamber. The sample is isolated from the deposition sources by a series of shutters. The primary shutters are integrated into each of the six individual sputter guns which block the stream of material from exiting each gun. The secondary shutter covers the entire sample area and blocks the stream of material even if one or more of the individual gun shutters are opened. To produce a more uniform deposition the sample is rotated about a central axis throughout the deposition process.

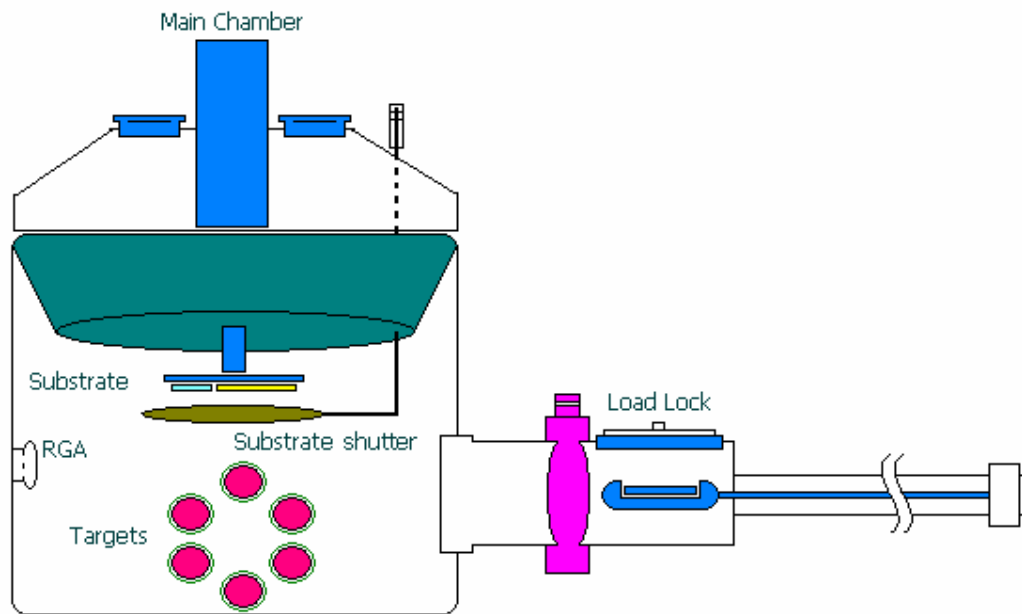


Figure 3.3 Reactive Magnetron Sputtering System.

3.2 The Deposition Process

The vacuum condition of the main chamber is critical to the outcome of the thin film depositions. For this reason prior to any deposition, the chamber is pumped down to less than 5.0×10^{-8} Torr. In this pressure range most contaminants are eliminated.

. To accurately control the percentage of oxygen present in the chamber a mixed gas consisting of 20% oxygen in argon is supplied through one mass flow controller and is diluted with 100% argon gas supplied by a second mass flow controller. To calculate the flow rate of the mixed gas the following formula is used.

$$D = \frac{X_i * A_i}{0.2 - 0.8 * X_i} \quad (3.1)$$

The equation above was used to calculate the flow of 20% oxygen in argon mixture in single vanadium target deposition. In the equation D represents the flow rate of 20% oxygen in argon mixture, X_i is the oxygen's percentage desired and A_i is the fixed 100% argon flow.

Having determined the desired mixed gas flow one can begin the process. The process is started with allowing the oxygen and argon to flow until the flow and the chamber pressure stabilize. Once the gas is stabilized, the gun is turned on. When this occurs the reaction between oxygen and the vanadium cause the percentage of oxygen to fall off. This is illustrated in figure 3.4. When the power is not yet applied to the target, the percentage of oxygen is proportional to the flow rate of oxygen. However, when power is applied to the target, much of the oxygen is consumed to form vanadium oxide. The decrease in the percentage of free oxygen inside the chamber was shown in figure 3.4. For example, a flow of 5 sccm yielded 2.5% of oxygen when the gun was off. However, this percentage of oxygen dropped down to 0.4% when the power is

turned on to the target. Hence, by controlling the flow rate at a constant rate of vanadium metal deposition, we can now control the percentage of oxygen inside the chamber during the deposition process.

For each deposition run, two substrates were coated, silicon with 300 nm of SiO₂ and a glass slide with 3 liftoff lines. The substrates are mounted on a holder that is transferred between the load lock and the main chamber. The samples are then deposited with vanadium oxide and removed for evaluation.

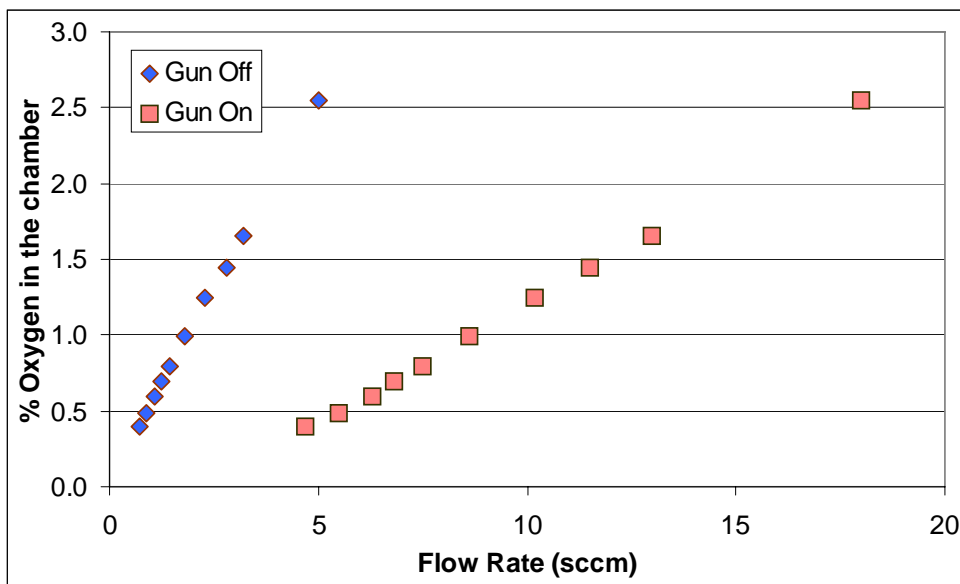


Figure 3.4 Reaction Between Oxygen and Vanadium.

3.3 Sample Preparation

To determine the properties of the amorphous vanadium deposition the electrical characterization performed on the thin films included resistivity and TCR measurements, as well as mechanical thickness. In order to calculate resistivity, the thickness and sheet resistance of the VO_x films have to be determined. For the thickness measurement, the sample was prepared as figure 3.5 illustrates. Glass slides are used as substrates and were thoroughly cleaned prior to deposition. On the surface of the glass slide, 3 ink lines are drawn using a permanent marker. The VO_x thin films were deposited on top of the marker lines. The glass slides are then immersed in acetone for a short duration to lift off the VO_x on the region with the ink lines, thus creating a step, which was then used for film thickness measurements.

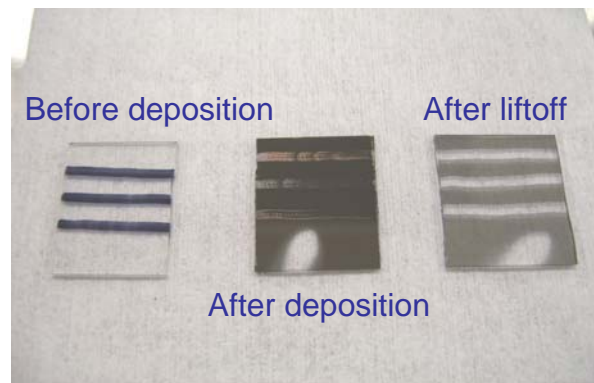


Figure 3.5 Sample Preparations for Thickness Measurement.

Sheet resistance is measured using the silicon wafer sample and requires no pre-measurement preparation. A typical silicon substrate with VO_x thin film deposition is in figure 3.6.

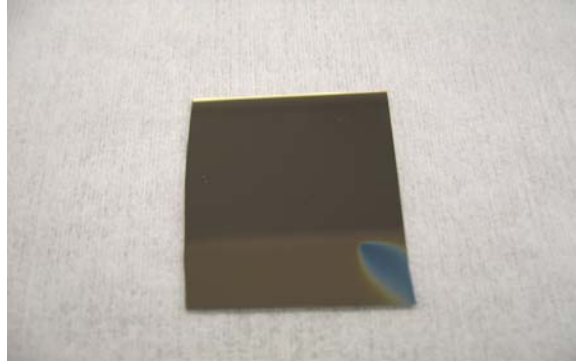


Figure 3.6 Sample Preparations for Sheet Resistance Measurement.

TCR sample preparation is more challenging as shown figure 3.7. A small portion of the silicon substrate is cut off and used for TCR measurements. Wires are mounted to the surface of the substrate using a metal epoxy which is electrically conductive. Current is injected by the outermost wires and voltage is sensed by the finer inner wires. The use of different wire sizes improved the accuracy of the measurement by providing improved mechanical attachment for the current sources and minimizing the area of voltage sensing

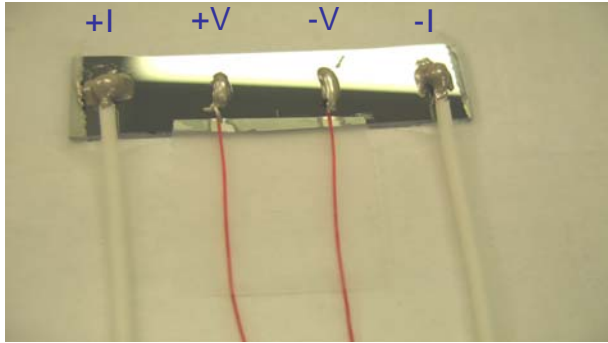


Figure 3.7 Sample Preparations for TCR Measurement.

3.4 Measurements

To measure the thickness of the deposited films a Dektak III profilometer was used. The glass slide with the trenches created in the sample preparation step is used for this measurement. The stylus is scanned from the surface of the vanadium oxide thin film to the glass slide surface as figure 3.8 illustrated. There are total of 3 measurements taken from each of the trenches on the glass substrate. The final result for the thickness measurement is the average of the three. With this technique, the surface uniformity of the vanadium oxide can also be estimated.

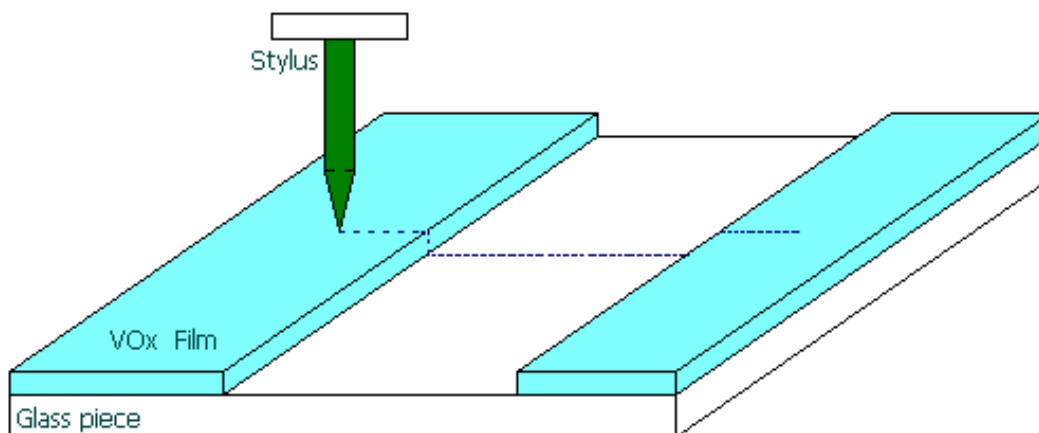


Figure 3.8 Thickness Measurement Technique.

For sheet resistance measurement, a 4 point probe, Jandel Model RM3, is used. This instrument can measure very high sheet resistance due to a wide range of current sources. The control panel allows the user to manually enter the current setting and display the sheet

resistance result according to the current set. The current can be set to few hundreds of nano Amperes allowing vanadium oxide with high sheet resistance to be routinely measured.

Throughout the experiments a wide range of sheet resistance was encountered. Some VO_x films' sheet resistance was as low as 50Ω to a maximum around $3\text{M}\Omega$. Therefore, the current setting has to be selected for the particular measurement range. The relatively large surface area of the sample allowed for multiple sheet resistance measurements to be made then averaged to yield final sheet resistance number.

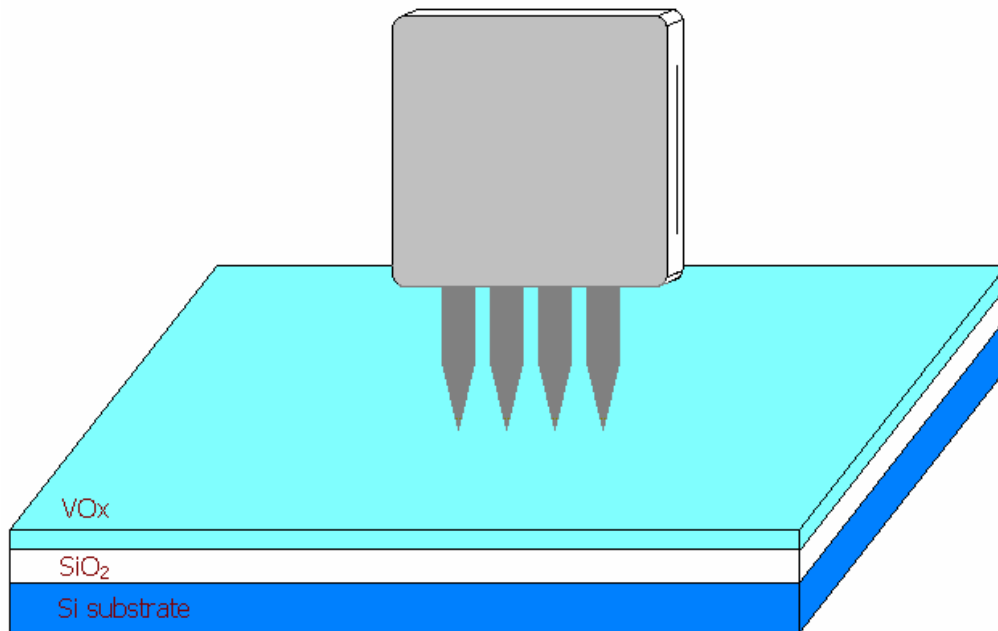


Figure 3.9 Sheet Resistance Measurement Technique.

Unlike the other two measurements, TCR measurement is much more complicated. Figure 3.10 illustrates the basic setting for TCR measurement. The TCR sample was placed on the surface of the hot plate with the addition of a thermal conductive compound to provide

adhesive and good thermal transfer between the two. The wires were connected to the current source / voltage meter which measures the resistance of the film. A thermocouple was placed on the surface of the film to measure its temperature. The temperature range for TCR measurement is about 2° C, referenced to room temperature. There are total of 350 data points recorded for 2° C, thus small fractions of temperature changed can be measured with respect to resistance. This method allows us to understand the sensitivity of the film with respect to temperature.

Both temperature and resistance data were recorded by use of a PC-based data acquisition system which was also used to calculate sample's TCR value. After each TCR measurement is completed, the temperature of the hot plate is cooled back down to room temperature prior to the next measurement. A fan and alcohol wipes are used to accelerate the cooling process. To summarize, a total of 3 TCR measurements are made for each sample and averaged for the final TCR value.

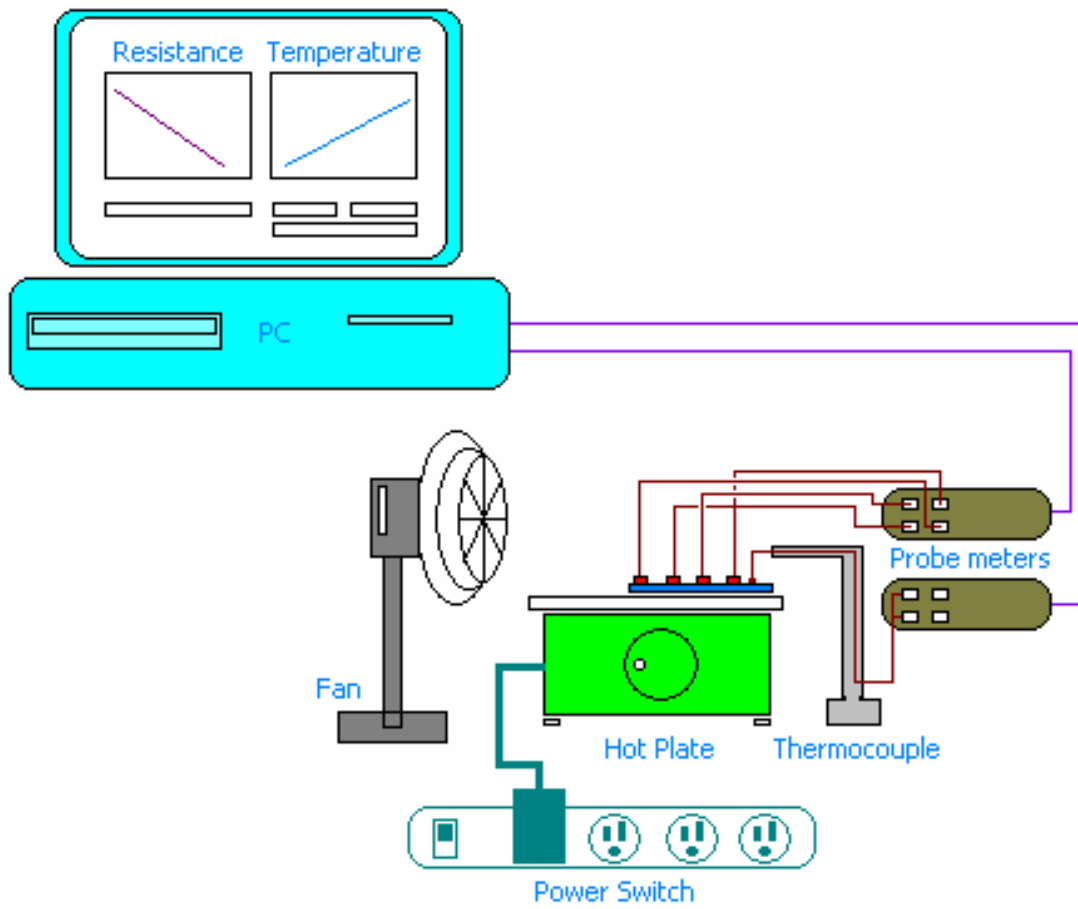


Figure 3.10 Temperature Coefficient of Resistance Measurement System.

3.5 Improvements

During the development of a vanadium oxide experimental process, the measurement values occasionally showed unexpected values. Thickness and TCR measurement techniques were suspected as the sources of these errors. For thickness sample preparation, the surface smoothness is very crucial. If the glass slide's surface is contaminated prior to deposition, the steps created after liftoff will be poorly generated. This can provide inaccurate results for the thickness measurement. In order to prevent this error, the glass slide surface was cleaned thoroughly to eliminate as much contamination as possible. In addition, the liftoff technique was improved to provide sharper steps by using a droplet to push a strong stream of acetone at the trench area to break the thin film.

Problems from unexpected TCR measurement results were more difficult to solve. Not only is this more complicated equipment setting, but it is also more difficult to controlling the measurement process. One of the most crucial parameters for the measurement is the temperature rising rate. In order to have accurate and repeatable measurement, the temperature rising rate has to be constant throughout each run. However, achieving a constant temperature rising rate is very challenging.

After the TCR measurement is completed, it is very difficult to get the hot plate's temperature back to room temperature. Even though the fan and alcohol wipes removed most of the heat from the hot plate, some partial heat is still trapped inside the hot plate's surface. Initially, room temperature seems to be obtained by using this technique. However, after 10 minutes, the temperature will start rising slowly due to the heat of previous run. This trapped

heat can take very long time for a complete removal. To solve this problem, equilibrium temperature needs to be achieved.

A modified cooling technique was used to remove majority of the heat; however, cooling was continued until the temperature was below room temperature. The residual heat from the previous cycle was allowed to equilibrate for about 15 minutes, during which time the temperature reading was continuously monitored. When the temperature reading showed a constant value for a long duration of time, an equilibrium temperature was achieved. With this method, every measurement starting point was similar and the temperature rising rate during measurement was constant for every measurement run.

CHAPTER FOUR: RESULTS AND DISCUSSION

4.1 Experiments Summary

Our work on amorphous vanadium oxide deposited using DC magnetron sputtering technique can be categorized into 3 main experiments. The first experiment developed amorphous VO_x thin films using a single vanadium target sputtered in different concentration of oxygen in the deposition chamber. Resistivity and TCR measurements were performed to characterize the electrical properties of amorphous VO_x thin films. The second experiment used noble metals to co-sputter along with single vanadium target. This method allows the resistivity of VO_x thin films to be reduced and was intended to understand the effects of noble metal additions on TCR values. The third experiment used 4 vanadium targets sputtered simultaneously to deposit VO_x thin films. This method increases the reactive metal deposition rate which allows better control of oxygen concentration in the deposition chamber. In addition, a liquid nitrogen cryo-trap was also applied with this technique to reduce sensitivity to chamber background gas. The experiments were performed in this order such that the results of the previous experiment served to guide for the next experiment.

4.2 Single Vanadium Target Depositions

The first set of sample depositions was performed with small concentrations of oxygen, in the range of 0.025% to 3.000%. The deposition time was 8 minutes and operating pressure was at 4 mTorr. The overall film thickness was about 500 Angstroms and the film sheet resistances are increase with the percentages of oxygen applied during deposition. Table 4.1 included the samples' data for single vanadium target deposition experiment.

Table 4.1 Single Vanadium Target Deposition Data.

% of O2	Thickness (m)	Rs (Ω / sq)	Resistivity (Ω-cm)	TCR (%/$^{\circ}$C)
0.04087	4.36E-08	292.54	0.00128	-1.2966
0.04431	5.12E-08	1204.61	0.00617	-1.7738
0.07323	4.32E-08	10687.14	0.04617	-0.2197
0.09451	5.07E-08	132082.87	0.66966	-2.8318
0.14999	3.20E-08	246590.65	0.78909	-1.7716
0.30335	4.71E-08	536374.22	2.52161	-2.7765
0.30344	5.27E-08	556130.78	2.93081	-2.4995
0.40098	5.71E-08	594249.44	3.39316	-2.7229
0.49000	4.32E-08	659338.02	2.84834	-2.8732
0.59253	5.00E-08	769964.14	3.84982	-4.4451
0.61509	5.90E-08	684812.39	4.04039	-4.0521
0.69664	5.28E-08	770294.98	4.06716	-2.7551
0.99024	4.30E-08	954121.96	4.10272	-3.0605
1.24539	4.75E-08	1096653.36	5.20910	-5.2249
1.43957	5.60E-08	1222824.24	6.84782	-3.5845
1.65512	4.74E-08	1400478.64	6.63827	-2.0754
1.99691	5.28E-08	1443260.72	7.62042	-3.7908
2.54525	4.31E-08	2546884.30	10.97707	-1.8253
3.14118	5.51E-08	3399271.92	18.72999	-1.6736

The sheet resistance values increase corresponding to the increase of oxygen percentage in the chamber. Figure 4.1 illustrate the relationship of resistivity with respect of percentages of oxygen in the chamber. In the range of higher percentages of oxygen, from 0.5% to 3.0%, the resistivity appears to have a small steady slope. However, when the percentages of oxygen decreased below 0.5% the slope increases dramatically. In this region, the resistivity is very difficult to control. Due to the limit of the mass flow control of the sputtering system, it is very difficult to control the oxygen concentration precisely at this low volume of flow. Thus, the stability of amorphous VO_x deposition was more stable at 0.5% oxygen or above.

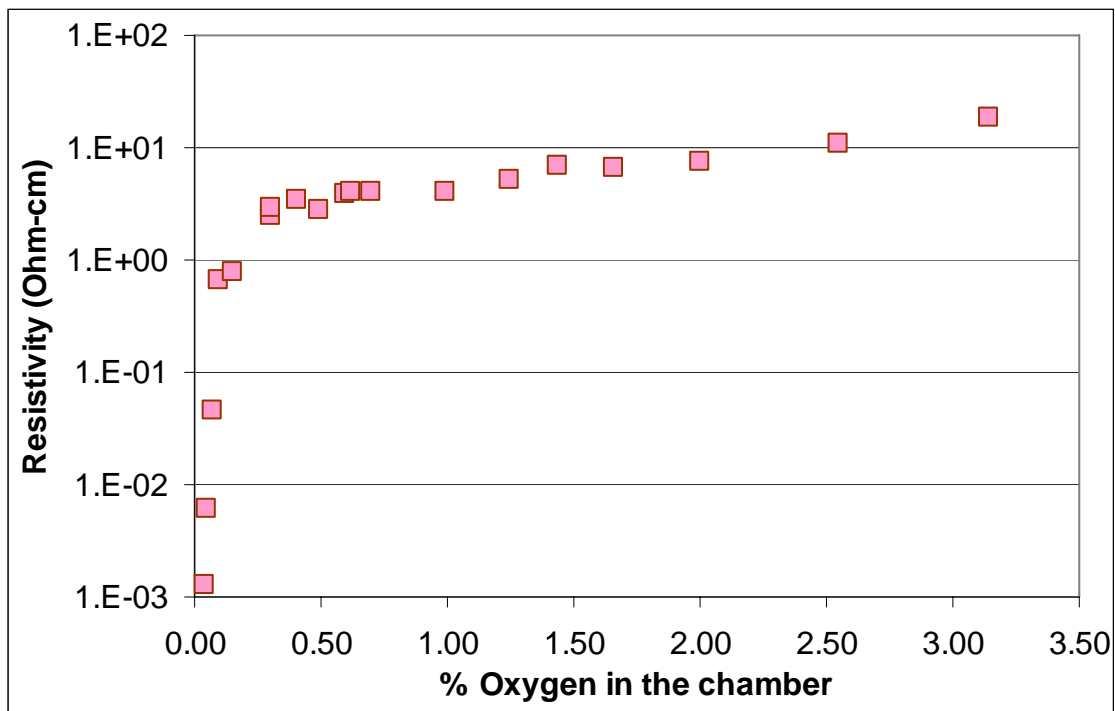


Figure 4.1 Resistivity vs. Percentages of O_2 in Single Vanadium Target Depositions.

The TCR values appear to be very scattered as oxygen concentration increased. Figure 4.2 displays the unexpected TCR values with respect to different percentages of oxygen in the chamber. Some samples appear to have very high TCR values (-5%) which are not consistent with values found in the literature. The TCR measurement technique was suspected to cause this error. This TCR data did approximate the expected trend with respect to resistivity, as shown in figure 4.3. The literature has found increased resistivity with increased TCR values in amorphous VO_x films as this experiment demonstrated. However, the unknown parameters were present during measurement to cause this inconsistency.

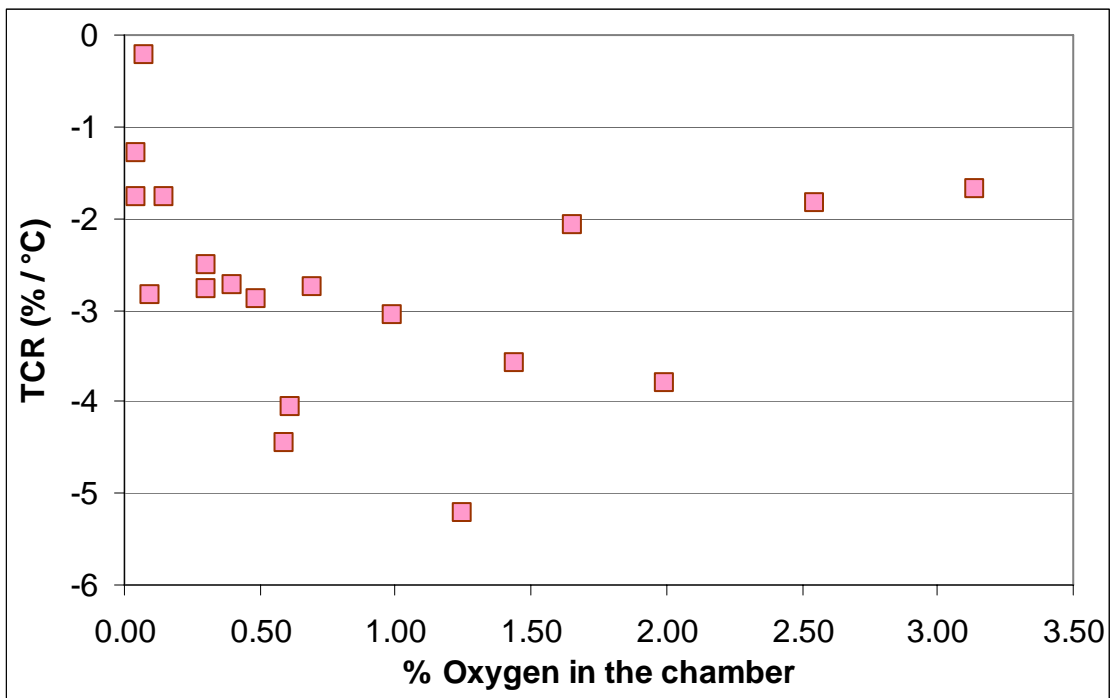


Figure 4.2 TCR vs. Percentages of O_2 in Single Vanadium Target Depositions.

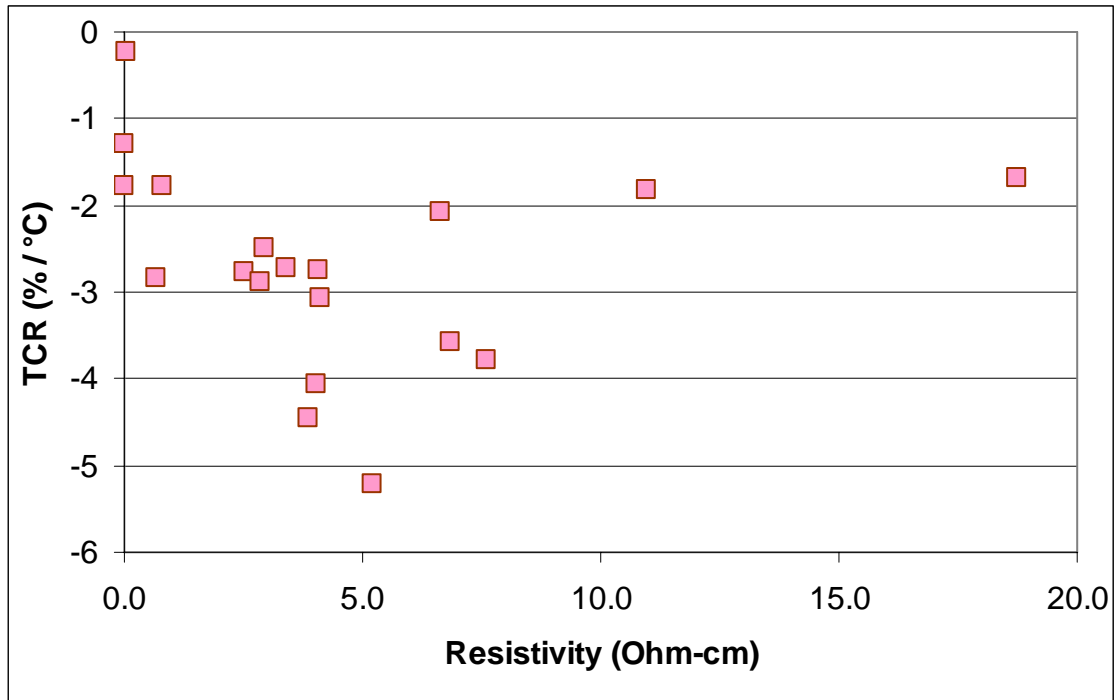


Figure 4.3 TCR vs. Resistivity in Single Vanadium Target Depositions.

In general, the first experiment had gives us some insights about the films' behavior, measurement techniques, as well as the development process. The results had demonstrated that VO_x thin films can be very sensitive at low percentages of oxygen thus affects the resistivity outcomes. In addition, a first wafer effect was observed during thin film depositions. With the same setting, the first and the second deposition of vanadium oxide films yielded different results, thus introducing another source of variability. From this we concluded that the chamber condition and background gas can also have an impact on films' properties.

Resistivity can be further reduced by introducing metallic regions inside the amorphous VO_x thin films, forming a nanocomposite thin film. Figure 4.4 illustrate the theory of metal additions to amorphous VO_x thin film. Metal clusters inside the film can act as a short, which

reduces the resistivity. The composite resistivity is still determined by that of the VO_x and should still maintain the TCR value of the vanadium oxide thin film. An experiment was carried out at 0.5% of oxygen in the chamber because it has low resistivity and the most stable TCR values according to the previous experiment data.



Figure 4.4 Metal Additions to Amorphous VO_x Thin Film.

4.3 Noble Metals Co-Sputtered With Single Vanadium Target

A theory of metal additions vanadium oxide had been established to reduce the film's resistivity. However, its effect on TCR values is still unknown. The first chosen noble metal for this experiment was platinum. By using DC magnetron sputtering deposition technique, platinum can be sputter simultaneously with the vanadium target. By controlling the DC power of platinum, we can control the amount of platinum added to the vanadium oxide thin films. The resistivity of platinum additions to vanadium oxide films has showed a great reduction as shown in figure 4.5. However, the TCR values are also reduced as well. Figure 4.6 has showed that TCR values had dropped at least 2 %/°C when small amount of platinum incorporated in the film.

Base on this experiment, we found that platinum can improved VO_x film's resistivity; however, TCR values have suffered greatly. Platinum additions to vanadium oxide appear not to be an improved material for bolometer application as illustrated in figure 4.7.

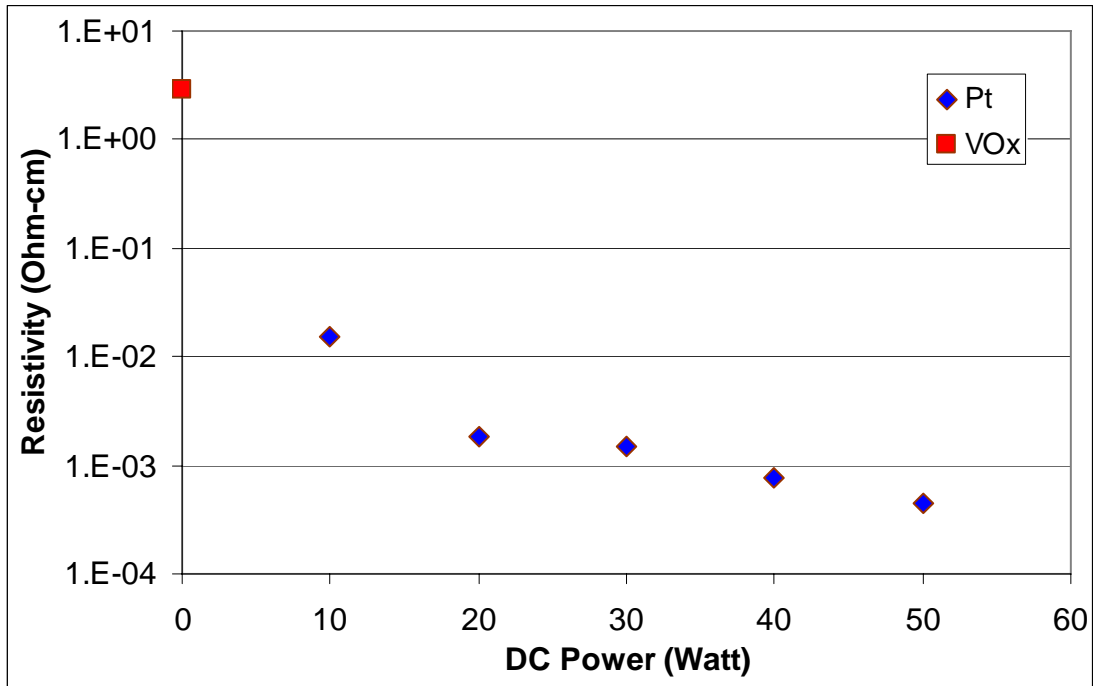


Figure 4.5 Resistivity vs. DC Power of Pt Additions VO_x Thin Films.

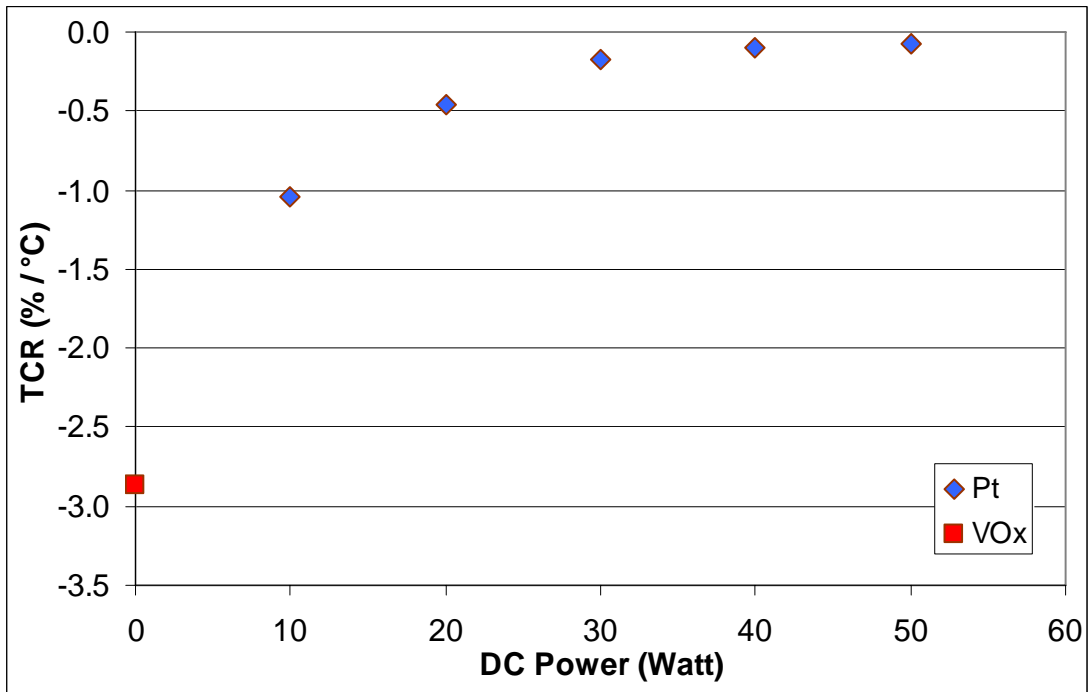


Figure 4.6 TCR vs. DC Power of Pt Additions VO_x Thin Films.

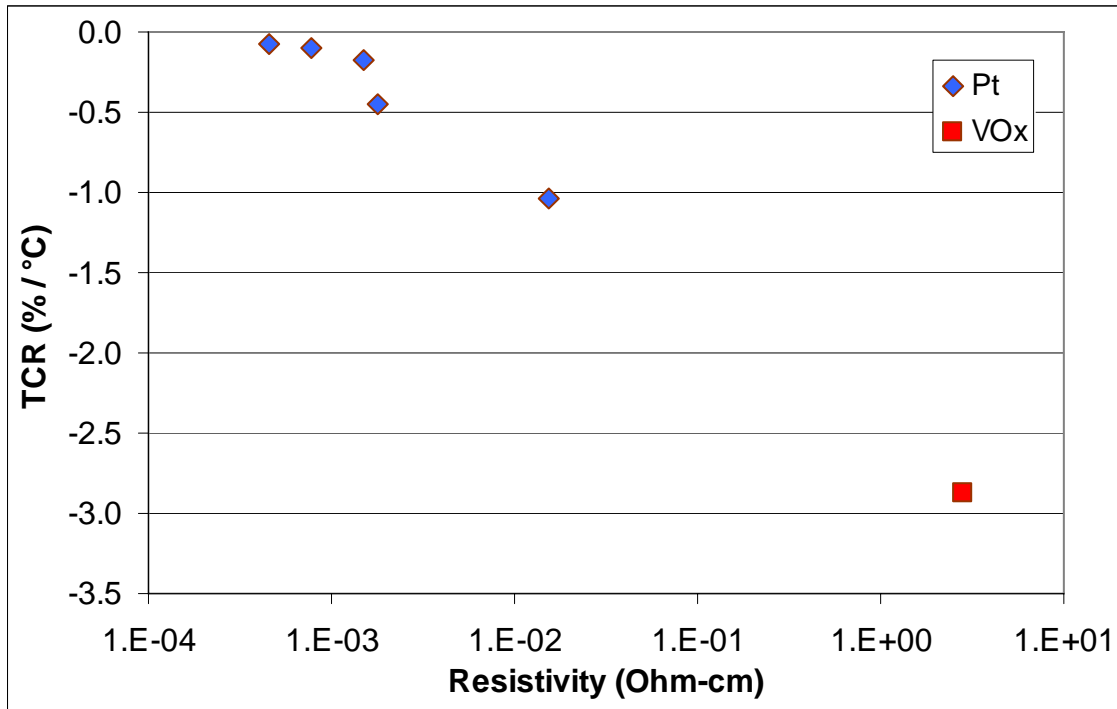


Figure 4.7 TCR vs. Resistivity of Pt Additions VO_x Thin Films.

The next noble metal that used to co-sputter with the vanadium target was gold. The deposition settings for gold are identical to platinum settings which were used for comparison purposes. The outcome of gold's resistivity with respect to DC power supply is illustrated in figure 4.8.

The resistivity of gold samples reduces gradually compare to the platinum samples which indicated gold has a better control in term of resistivity. While the resistivity of the gold samples did not drop as much as that of the platinum samples, TCR values of gold samples showed a much more promising result, as figure 4.9 illustrates.

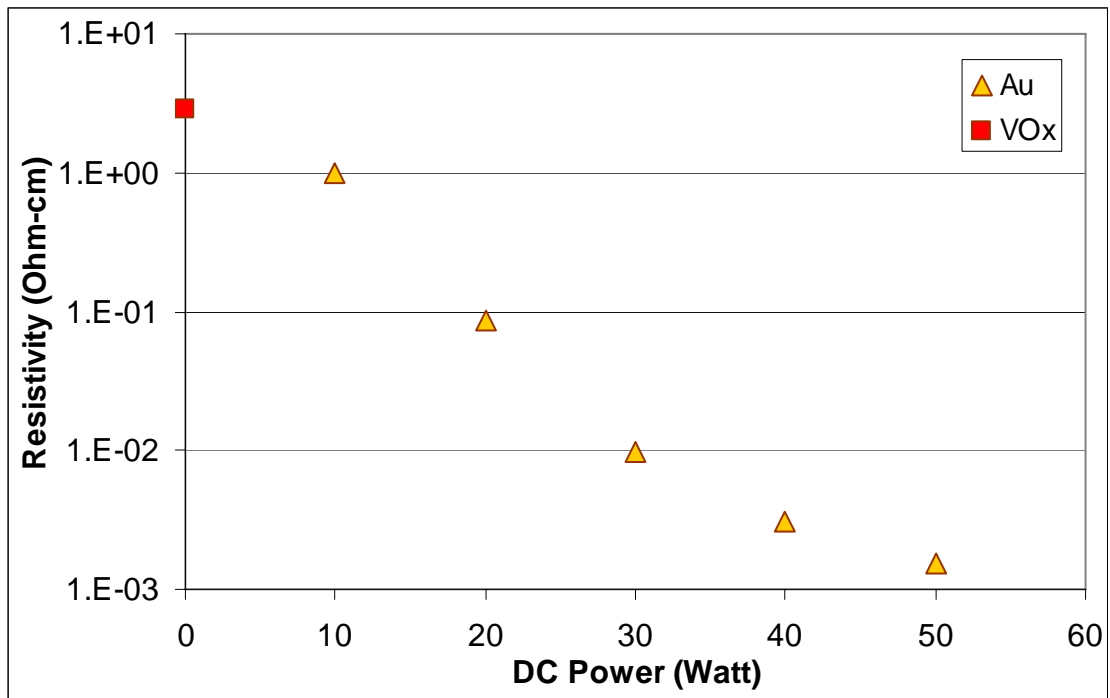


Figure 4.8 Resistivity vs. DC Power of Au Additions VO_x Thin Films.

The significantly, the initial TCR value for the smallest gold addition to VO_x sample was not reduced with respect to the pure vanadium oxide sample. This data showed that gold additions to vanadium oxide can improve resistivity and still maintain high TCR value, as figure 4.10 illustrates.

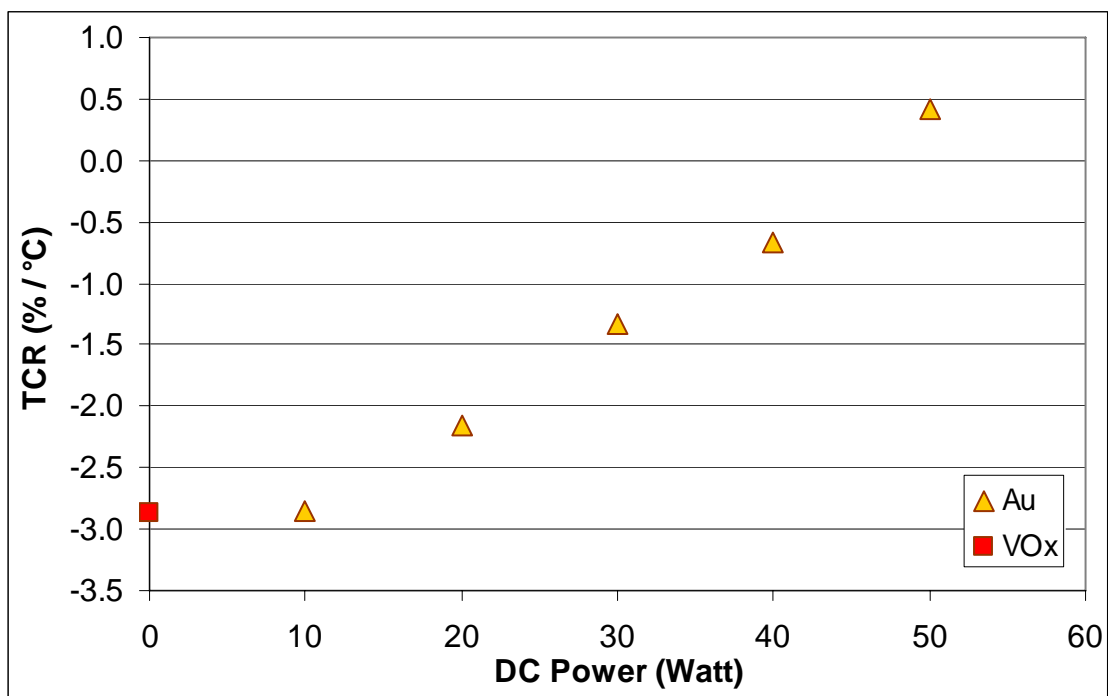


Figure 4.9 TCR vs. DC Power of Au Additions VO_x Thin Films.

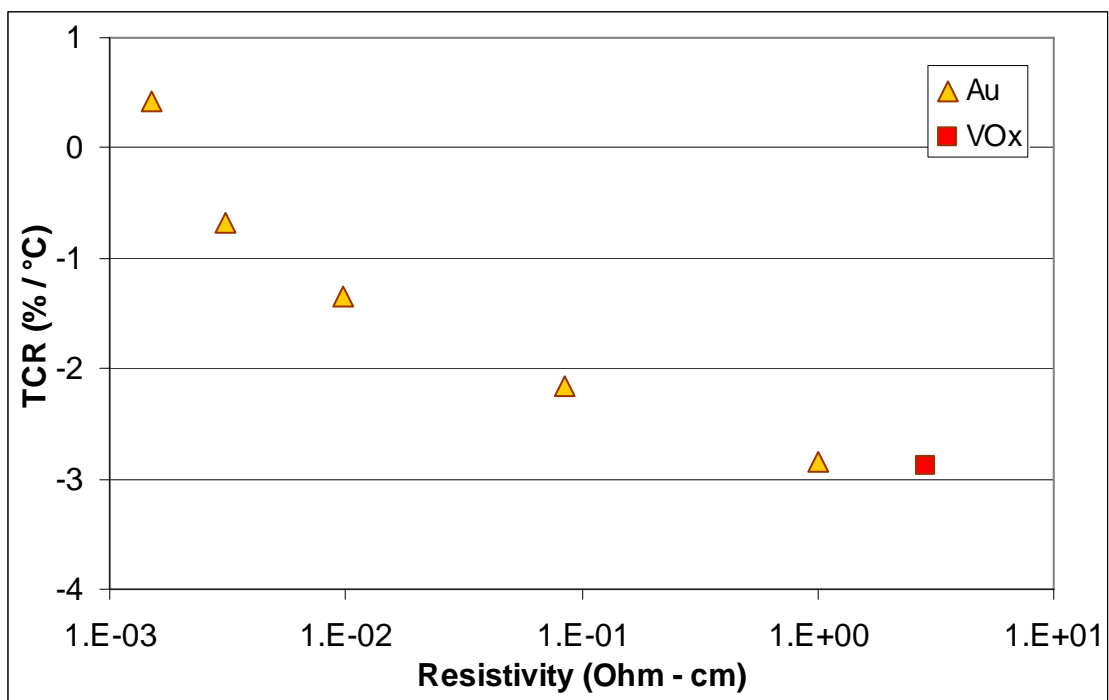


Figure 4.10 TCR vs. Resistivity of Au Additions VO_x Thin Films.

The theory of noble metals co-sputter with vanadium to deposit vanadium oxide was examined with platinum and gold additions. The results indicate both metals have different effects on vanadium oxide thin films. Platinum reduced resistivity greatly, but did not maintain high TCR values. Thus platinum is not a preferred metal to improve properties of bolometer thin films. Gold, on the other hand, reduced resistivity and maintained the high TCR values of the vanadium oxide thin films. By comparing the data of TCR with respect to resistivity of Zintu, et. al. [24], we can understand the advantages of gold additions to vanadium oxide thin films. Figure 4.11 shows gold samples have better TCR values and/or lower resistivity with respect to Zintu, et. al.. With this data, gold appear to be a preferred metal to improve the properties of amorphous VO_x thin films.

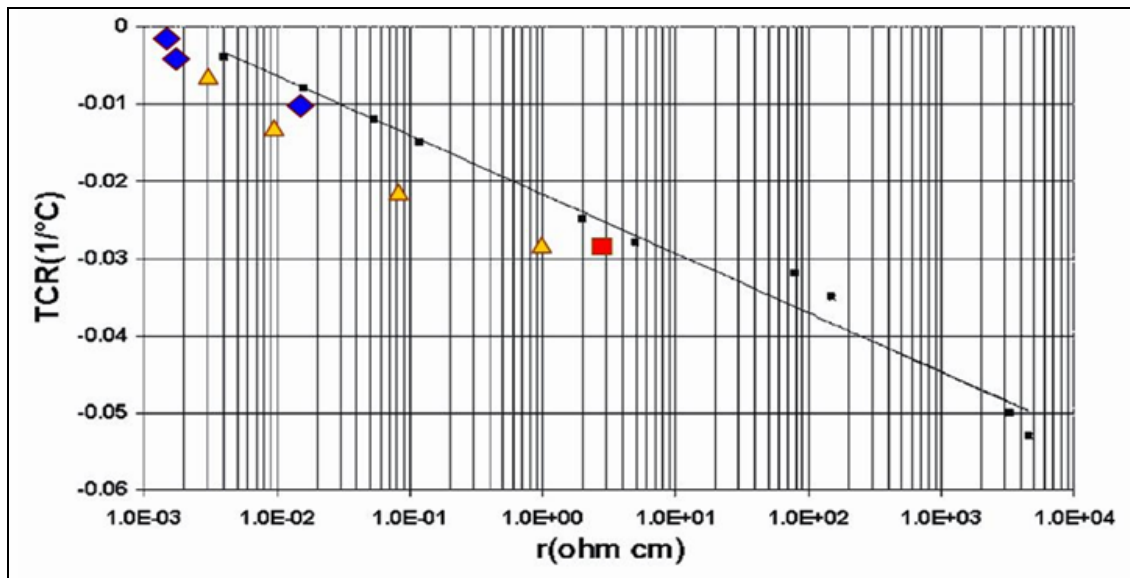


Figure 4.11 TCR vs. Resistivity of Pt and Au Addition VO_x with Respect to Zintu, et. al..

In order to confirm the gold data is correct and reproducible, another set of gold addition samples was generated. The resistivity of the second gold series showed a gradually decrease, similar to the first gold series. However, TCR values of the second gold series showed a different trend. Figure 4.12 and 4.13 illustrate the resistivity and TCR values vs. the DC power applied to sputter the gold target. The TCR values of the second gold series were not consistent with the first series. DC power applied to gold at 5, 10, and 15 Watts show an opposite trend compared to the rest of the samples. The TCR measurement technique was suspected to cause this error.

Both gold series were re-measured in term of TCR; and during this process, the improved technique for TCR measurement was developed and established. The inconsistency of TCR values was caused by the variation in the residual heat within hot plate at the start of each measurement run. By removing all excess heat, equilibrium temperature was achieved. Thus provided improved consistency for all the TCR measurements.

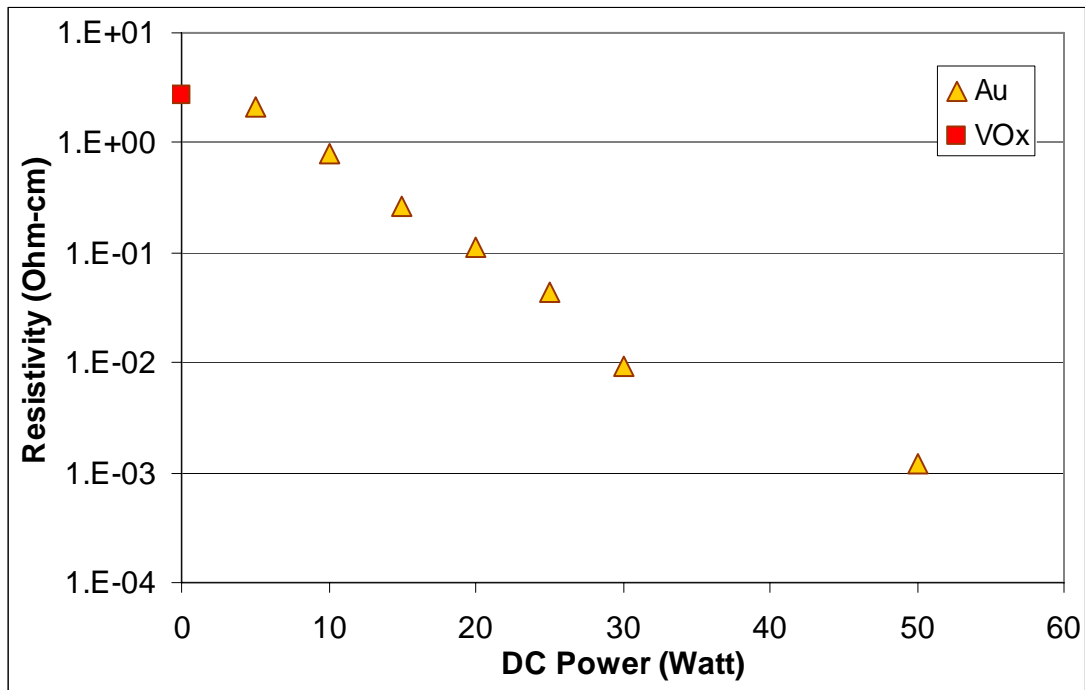


Figure 4.12 Resistivity vs. DC Power of 2nd Au Additions VO_x Thin Films.

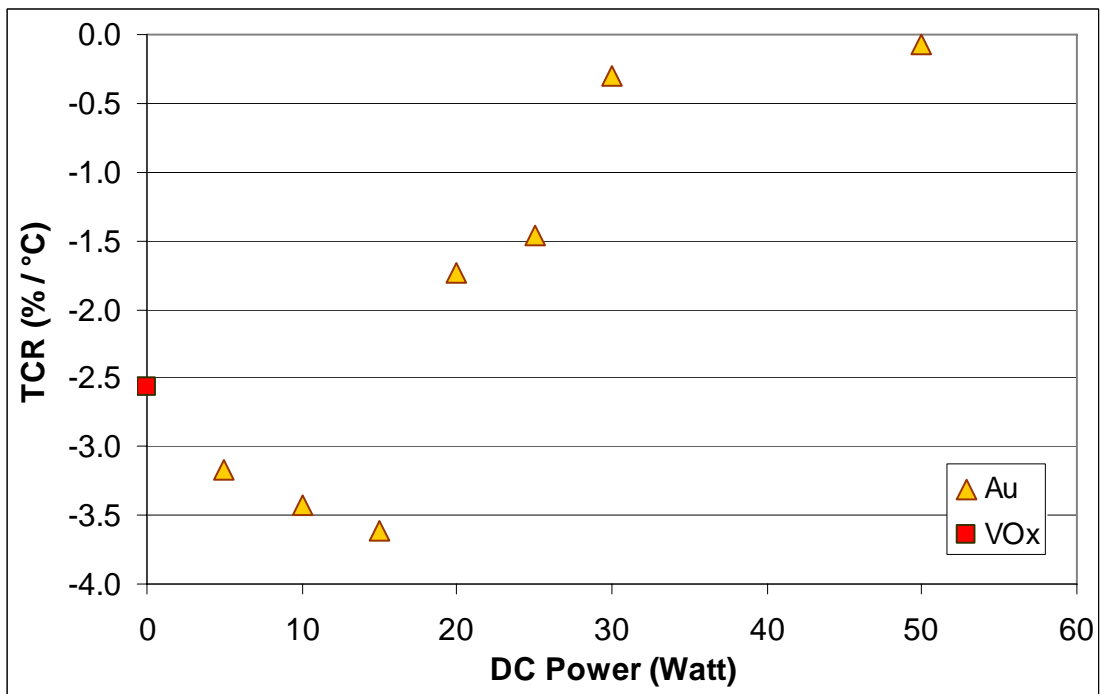


Figure 4.13 TCR vs. DC Power of 2nd Au Additions VO_x Thin Films.

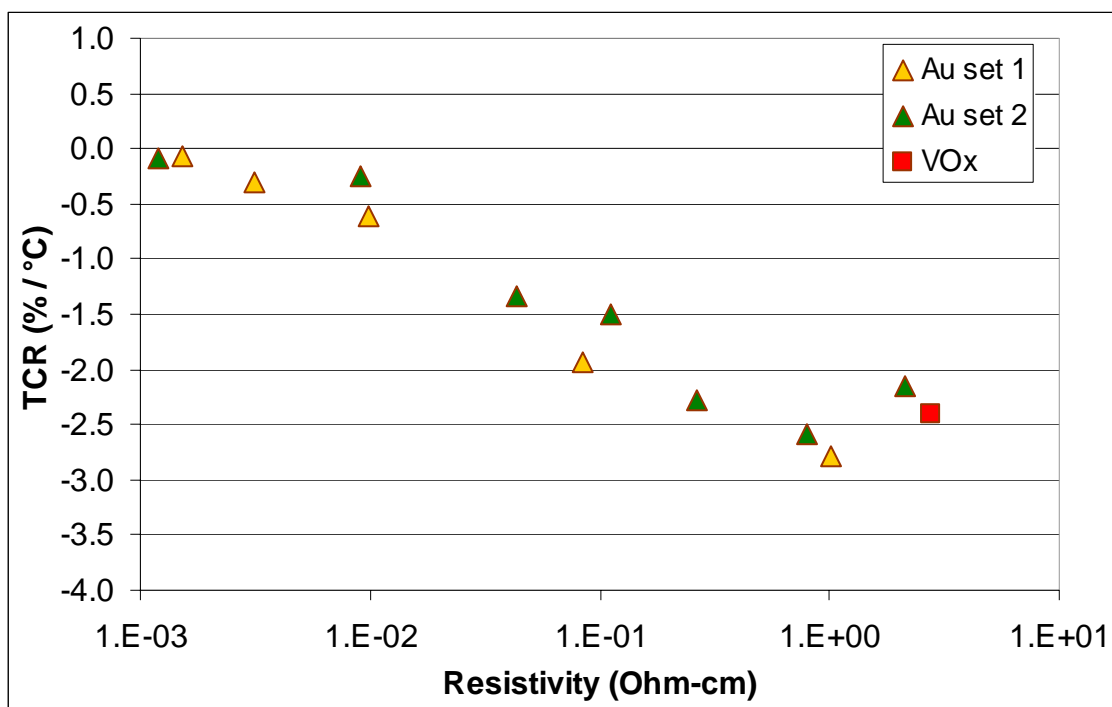


Figure 4.14 TCR vs. Resistivity of 1st and 2nd Au Additions VO_x Thin Films.

Figure 4.14 confirmed the improved TCR measurement technique provides the ability to reproduce the data for both gold sample series. The resistivity for both series match closely and the TCR values for both have a significantly reduced variation.

For both series, 10 Watts of DC power for gold yielded the highest TCR and the lowest resistivity comparing to the amorphous vanadium oxide sample. We can compare the results of the two gold series with that of Zintu, et. al.. [24] as figure 4.15 illustrates. The repeatability of gold additions amorphous vanadium oxide was successfully established with the additional improved values in term of TCR and resistivity. The data from these experiments is summarized in table 4.2.

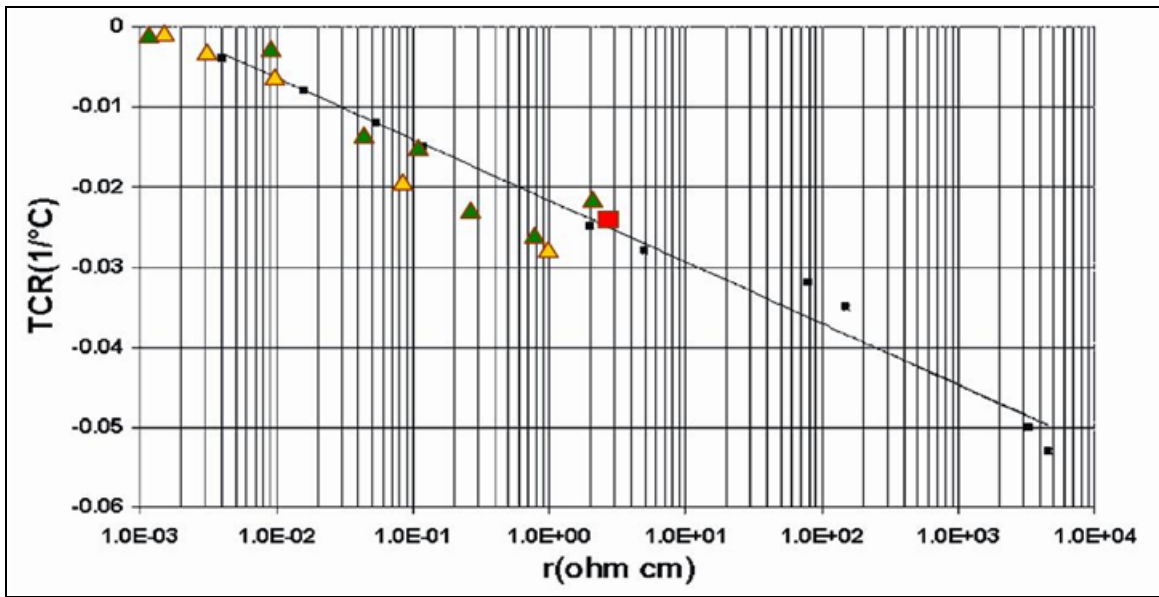


Figure 4.15 TCR vs. Resistivity of 1st and 2nd Au Additions VO_x with Respect to Zintu, et. al..

Table 4.2 Noble Metals Co-Sputter Single Vanadium Target Depositions.

Samples	Thickness (m)	Rs (Ω / sq)	% of O2	Resistivity (Ω-cm)	1st TCR (%/°C)	2nd TCR (%/°C)
050806 A (10W Pt)	3.56E-08	4291.58	0.5	0.01528	-1.0410	
050806 B (20W Pt)	2.83E-08	635.16	0.5	0.00180	-0.4540	
050806 C (30W Pt)	7.40E-08	204.42	0.5	0.00151	-0.1732	
050806 D (40W Pt)	7.48E-08	104.58	0.5	0.00078	-0.1017	
050806 E (50W Pt)	7.54E-08	59.82	0.5	0.00045	-0.0703	
081806 A (10W Au)	5.20E-08	193400.83	0.5	1.00568	-2.8470	-2.7827
081806 B (20W Au)	5.59E-08	15189.45	0.5	0.08491	-2.1519	-1.9284
081806 C (30W Au)	8.63E-08	1133.41	0.5	0.00978	-1.3388	-0.6174
081806 D (40W Au)	1.12E-07	277.86	0.5	0.00311	-0.6729	-0.3001
081806 E (50W Au)	1.23E-07	123.19	0.5	0.00151	0.4213	-0.0608
082306 A (00W Au)	4.18E-08	660017.82	0.5	2.75887	-2.5723	-2.4043
082306 B (05W Au)	4.64E-08	460300.13	0.5	2.13579	-3.1707	-2.1540
082306 C (10W Au)	4.44E-08	178742.08	0.5	0.79361	-3.4223	-2.5910
082306 D (15W Au)	5.71E-08	46489.48	0.5	0.26545	-3.6166	-2.2824
082306 E (20W Au)	6.11E-08	18293.42	0.5	0.11168	-1.7332	-1.4941
082306 F (25W Au)	7.81E-08	5597.36	0.5	0.04369	-1.4552	-1.3414
082306 G (30W Au)	7.54E-08	1213.17	0.5	0.00914	-0.2979	-0.2566
082306 H (50W Au)	1.28E-07	93.33	0.5	0.00120	-0.0681	-0.0836

Using noble metals co-sputtered with single vanadium target was a success in terms of finding a new technique to improve the properties of amorphous vanadium oxide. However, the single vanadium target deposition experiments still suffered problems such as the limit of mass flow control and variable chamber background gas. To overcome these limits, 4 vanadium targets were used simultaneously to sputter vanadium at a 4-fold higher rate. This technique increased the reactive metal deposition rate of vanadium which gained a better control of oxygen

concentration inside the chamber. In addition, sensitivity to chamber background gas was further reduced by implementing liquid nitrogen cryo-pumping technique.

4.4 Four Vanadium Targets Depositions

A reactive gas test was performed for the 4 vanadium targets depositions. Figure 4.16 demonstrates the single vanadium target and the 4 vanadium targets depositions oxygen flow rate with respect to percentages of oxygen in the chamber. By using 4 vanadium targets techniques, the flow rate is about 4 times higher compared to the single vanadium target deposition. For example, a single target at 10 sccm flow yields the same percentage of oxygen as 4 targets at 40 sccm. This technique allows higher flow rates to gain a better control of oxygen concentration inside the chamber. Due to the increased deposition rate of vanadium, the deposition time was reduced from 8 minutes to 3 minutes.

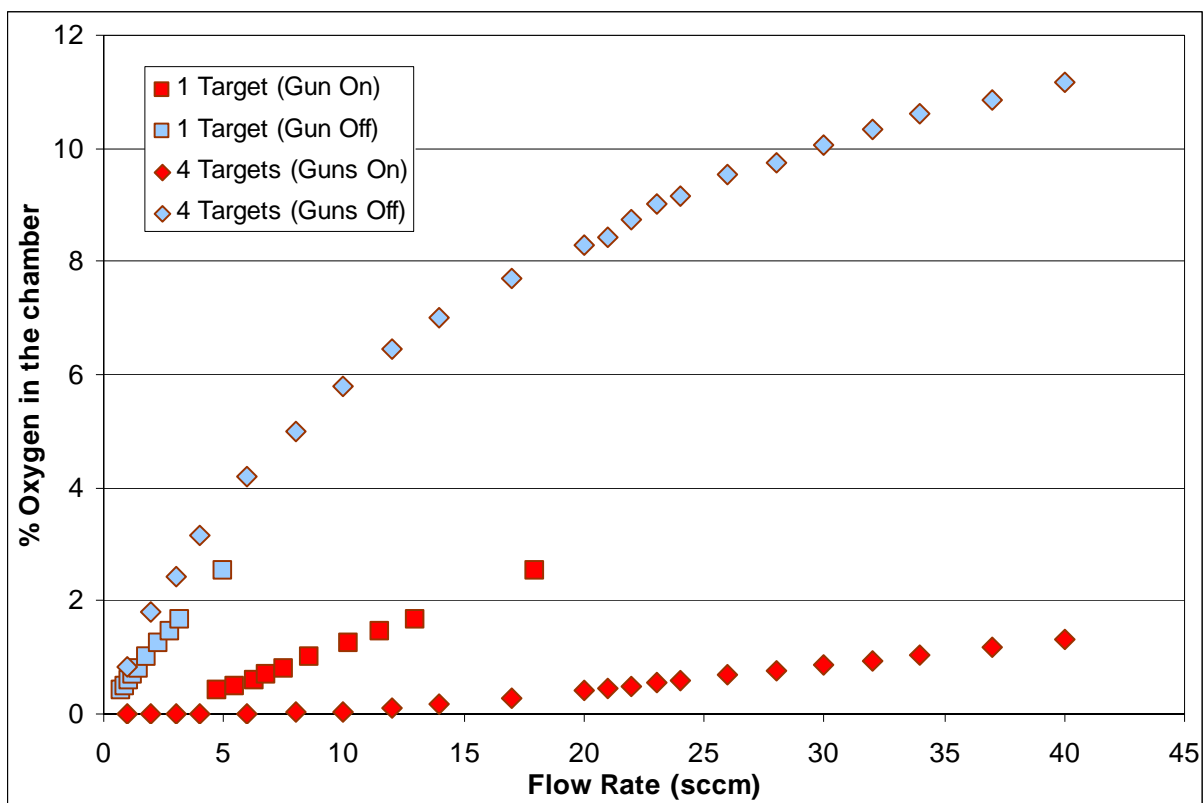


Figure 4.16 Reaction Rates of Oxygen and Vanadium for Single Target and Four Targets.

In order to reduce chamber background gas, a liquid nitrogen cryo-pumping technique was used. Figure 4.17 illustrated the percentages of oxygen with respect to flow rate with liquid nitrogen and without liquid nitrogen in the cryo-trap. The percentages of oxygen in the chamber showed no effect in either case. However, the resistivity of these two sample sets indicates an effect. In figure 4.18, the liquid nitrogen cryo-pump technique does affect the resistivity of the samples. The sample set with liquid nitrogen cryo-pump shows a higher resistivity than the sample set without liquid nitrogen cryo-pump. With figure 4.17 and 4.18, we do not understand why the liquid nitrogen cryo-pump technique increased the resistivity of the films. The major

effect is has on the chamber background gas is to reduce the amount of residual water vapor present in the chamber.

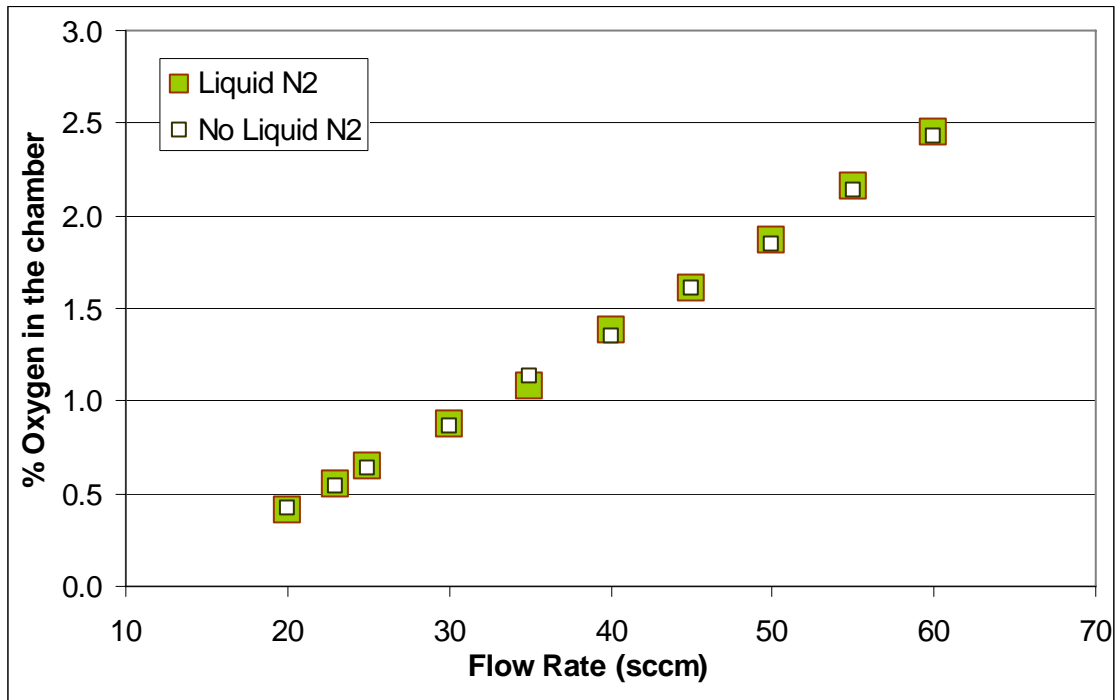


Figure 4.17 4 Vanadium Targets Deposition with and without Liquid Nitrogen Cryo-Pump.

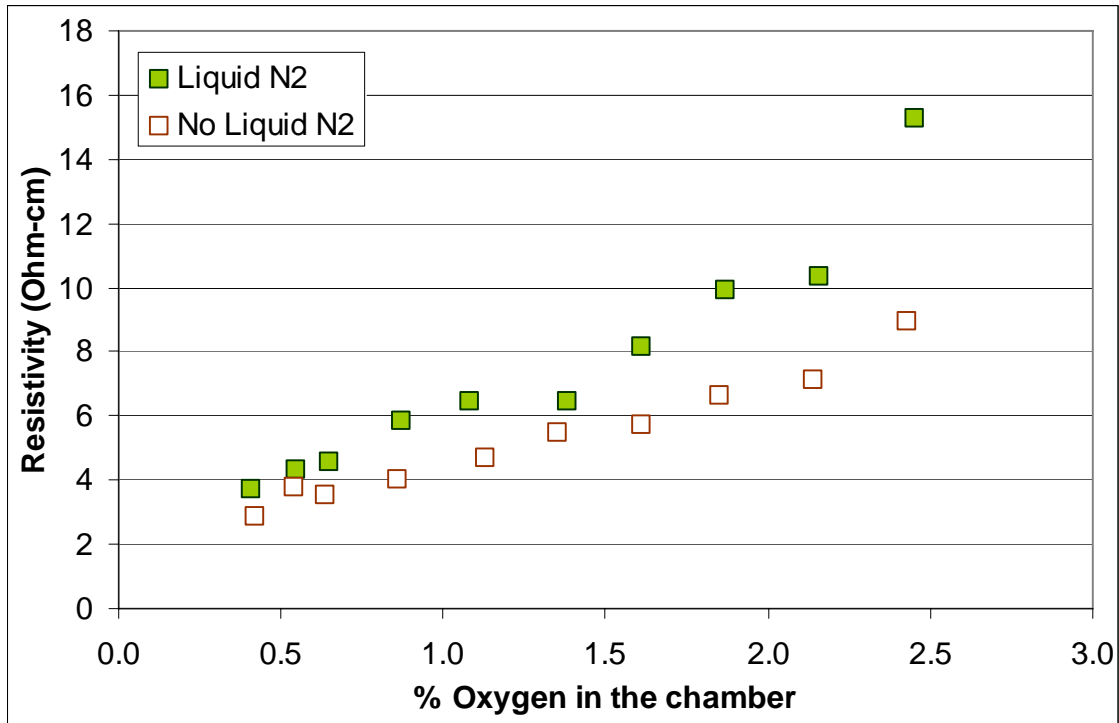


Figure 4.18 Resistivity vs. Percentages of O₂ for 4 Vanadium Targets Depositions.

TCR values for the 4 vanadium targets depositions showed a very interesting trend, as shown in figure 4.19. With decreasing percentages of oxygen, TCR values gradually increased. This data also confirmed our improved TCR measurement technique has reduced variability and yields more accurate results. Figure 4.20 displays the relationship between TCR with respect to resistivity for the 4 vanadium targets deposition experiment. In this figure, there is no obvious trend of TCR with respect to resistivity within this range of oxygen percentage. This data range is too small to claim that increased TCR with decreased resistivity for 4 vanadium targets depositions. However, by plotting this data with respect to Zintu, et. al., a new trend had vaguely recognized.

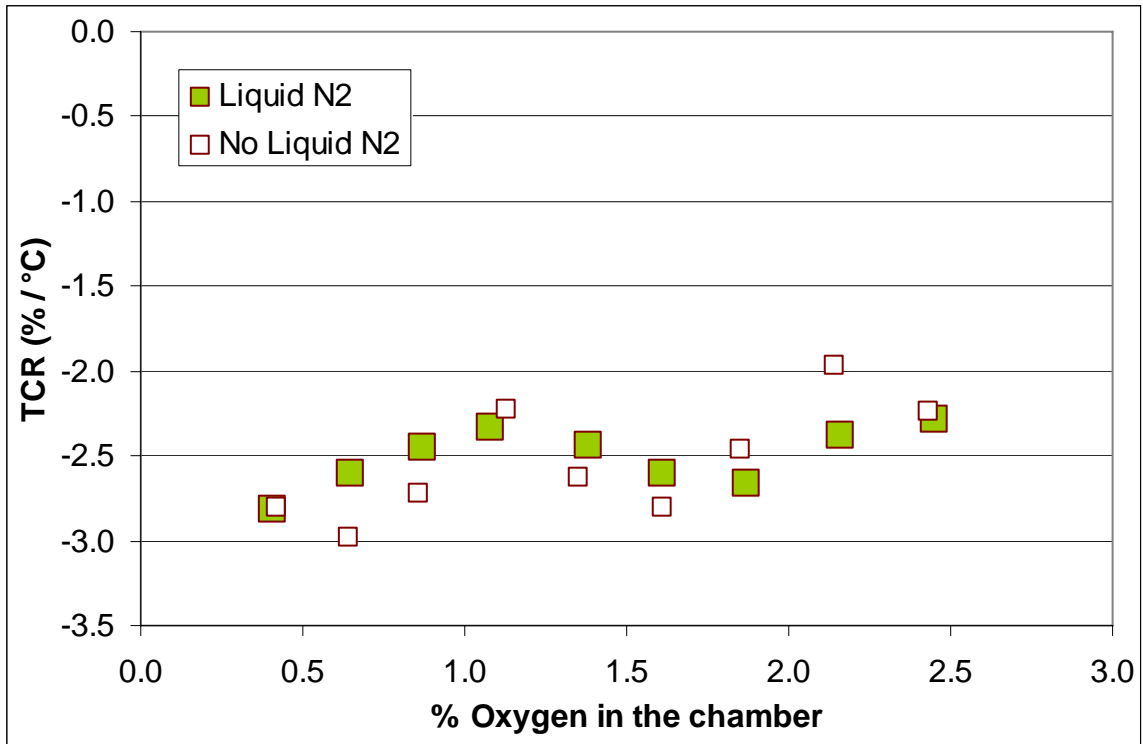


Figure 4.19 TCR vs. Percentages of O₂ in 4 Vanadium Targets Depositions.

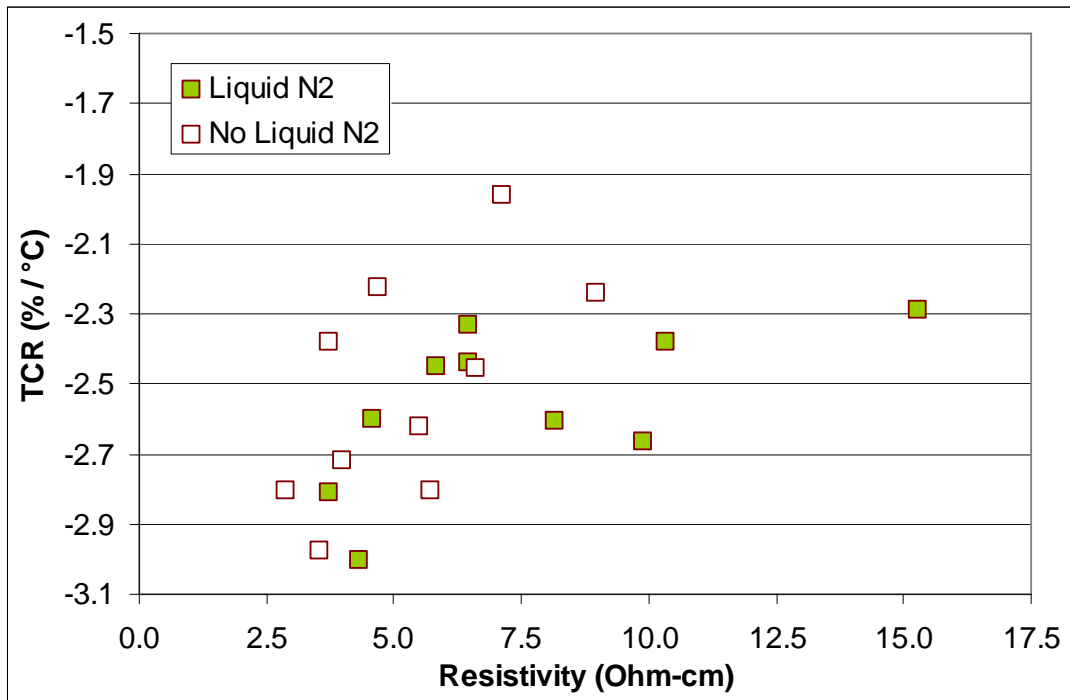


Figure 4.20 TCR vs. Resistivity in 4 Vanadium Targets Depositions.

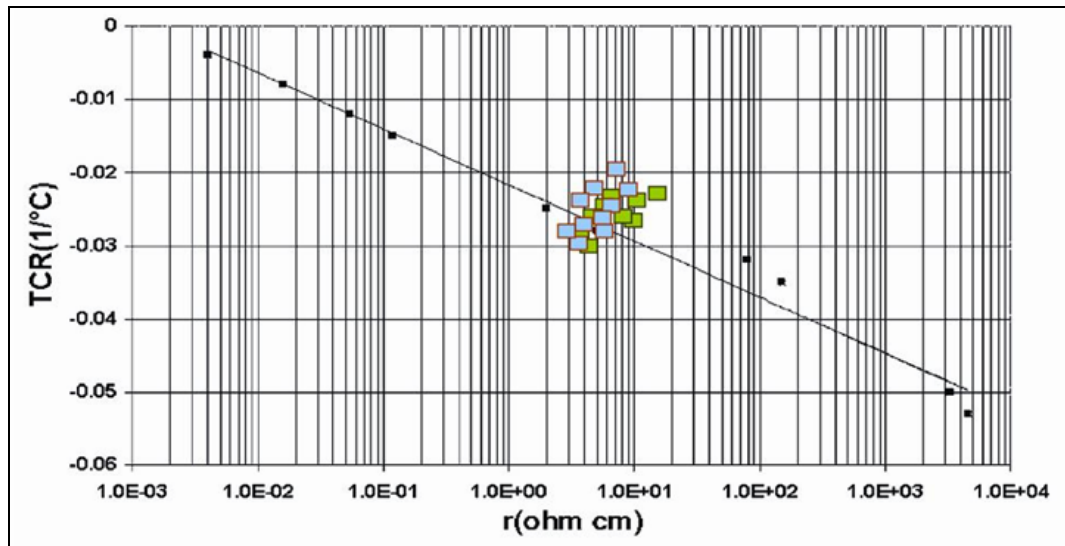


Figure 4.21 TCR vs. Resistivity in 4 Vanadium Targets Depositions with Respect to Zintu, et.

al..

In figure 4.21, 4 vanadium targets depositions seems to create a new relationship in term of TCR and resistivity. Instead of increased TCR with increase resistivity, the resistivity of 4 vanadium targets experiment is decreasing. This data trend is leading to an ideal bolometer thin film; however, it is too early to say due to a small range of resistivity. Table 4.3 includes all the measurement data from the 4 vanadium targets depositions.

Table 4.3 Four Vanadium Targets Depositions.

% Oxygen	Liquid N2	Tck (m)	Rs (kΩ/sq)	TCR (%/$^{\circ}$C)	Resistivity (Ω-cm)
2.45	Yes	7.52E-08	2032.167	-2.2919	15.28
2.16	Yes	6.93E-08	1492.000	-2.3828	10.34
1.87	Yes	7.82E-08	1264.225	-2.6649	9.88
1.61	Yes	7.35E-08	1110.925	-2.6050	8.16
1.38	Yes	6.80E-08	950.038	-2.4373	6.46
1.08	Yes	7.66E-08	843.540	-2.3329	6.46
0.87	Yes	7.58E-08	768.096	-2.4521	5.82
0.65	Yes	7.48E-08	612.478	-2.6019	4.58
0.55	Yes	7.93E-08	543.506	-3.0026	4.31
0.41	Yes	7.93E-08	470.941	-2.8113	3.73
2.43	No	6.94E-08	1291.583	-2.2408	8.96
2.14	No	7.07E-08	1005.388	-1.9625	7.11
1.85	No	6.81E-08	969.049	-2.4581	6.60
1.61	No	6.82E-08	838.338	-2.8022	5.72
1.35	No	7.67E-08	716.773	-2.6222	5.50
1.13	No	7.34E-08	640.639	-2.2245	4.70
0.86	No	6.70E-08	595.503	-2.7200	3.99
0.64	No	7.45E-08	477.237	-2.9773	3.56
0.54	No	7.95E-08	471.349	-2.3820	3.75
0.42	No	7.08E-08	406.063	-2.8023	2.88

CHAPTER FIVE: CONCLUSION

Vanadium oxide thin films have been successfully deposited using reactive magnetron sputtering deposition. The oxygen concentration was precisely controlled and measured during the depositions. A DC power supply was used to sputter vanadium metal targets in an oxygen / argon mixture at room temperature to develop amorphous vanadium oxide thin films.

The addition of gold to the vanadium oxide thin films was found to yield higher TCR and lower resistivity when compared to values reported in the literature, Furthermore, TCR measurement techniques have been established providing improved repeatability and accuracy. Vanadium oxide deposition using a four-target array appears to yield an increased TCR with a decrease in resistivity values, and results in an improved oxygen control technique. In summary, a novel nanocomposite bolometer thin film has been developed.

LIST OF REFERENCES

- [1] G. Stefanovich, A. Pergament, D. Stefanovich, “Electrical Switching and Mott Transition in VO₂”, *Journal of Physics Condensed Matter* 12 (2000) 8837 – 8845.
- [2] M. N. Gurnee, M. Kohin, R. Blackwell, N. Butler, J. Whitwam, B. Backer, A. Leary, T. Nielson, “Developments in Uncooled IR Technology at BAE SYSTEMS”, *Proc. SPIE* Vol. 4369 (2001) 287 – 296.
- [3] J. Anderson, D. Bradley, C. Chen, R. Chin, H. Gonzalez, R. Hegg, K. Koztrzewa, C.L. Pere, S. Ton, A. Kennedy, D. Murphy, M. Ray, R. Wyles, J. Miller, G. Newsome, “Advances in Uncooled Systems Applications”, *Proc of SPIE* Vol. 5074 (2003) 557 – 563.
- [4] H. Wada, M. Nagashima, M. Kanzaki, T. Sasaki, A. Kawahara, Y. Tsuruta, N. Oda, S. Matsumoto, “Fabrication Process for 256 x 256 Bolometer Type Uncooled Infrared Detector”, *SPIE* Vol. 3224, pp. 40-51.
- [5] D.S. Tezcan, S. Eminoglu, T. Akin, “A Low-Cost Uncooled Infrared Microbolometer Detector in Standard CMOS Technology”, *IEEE Trans. Elec. Dev.* Vol 50, No. (2003) 494 – 502.
- [6] C. Chen, X. Yi, J. Zhang, X. Zhao, “Linear Uncooled Microbolometer Array Based on VO_x Thin Films”, *Elsevier, Infrared Physics & Technology* 42 (2001) 87 – 90.
- [7] R.G. Cope, A.W. Penn, “High-Speed Solid-State Thermal Switches Based on Vanadium Dioxide”, *Applied Physics Ser. 2* Vol 1 (1968) 161 – 168.
- [8] S. Moon, “Novel Infrared Absorbing Material Coupled Uncooled Microbolometer”, *IEEE* (2004) 658 – 660.

- [9] Y. Dachuan, X. Niankan, Z. Jingyu, Z. Xiulin, “Vanadium Dioxide Films with Good Electrical Switching Property”, *Journal of Physics D: Applied Physics* 29 (1996) 1051 – 1057.
- [10] Y. Tanaka, A. Tanaka, K. Iida, T. Sasaki, S. Tohyama, A. Ajisawa, A. Kawahara, S. Kurasina, T. Endoh, K. Kawano, K. Okuyama, K. Egashira, H. Aoki, N. Oda, “Performance of 320 x 240 Uncooled Bolometer-type Infrared Focal Plane Arrays”, *Proc. SPIE Vol 5074* (2003) 414 – 424.
- [11] M. Soltani, M. Chaker, E. Haddad, R. Kruzelesky, “1x2 Optical Switch Devices Based On Semiconductor-to-metallic Phase Transition Characteristics of VO₂ Smart Coatings”, *Meas. Scil. Technol.* 17 (2006) 1052 – 1056.
- [12] Z.M. Wu, G.Z. Xie, H. Mu, T. Wang, J.H. Xu, C.H. Huang, Y.D. Jiang, “Study of Magnetron Sputtering of Vanadium Oxide Thin Films”, *IEEE 11th International Symposium on Electrets*, 2002.
- [13] Y. H. Han, K.T. Kim, H.J. Shin, S. Moon, “Enhanced Characteristics of an Uncooled Microbolometer Using Vanadium – Tungsten Oxide as a Thermometric Material”, *Applied Physics Letter* 86, 254101 (2005).
- [14] Y.H. Han, K.T. Kim, N.C. Anh, H.J. Shin, I.H. Choi, S. Moon, “Fabrication and Characterization of Bolometer Oxide Thin Films Based on Vanadium – Tungsten Alloy”, *Elsevier, Sensors and Actuators A* 123-124 (2005) 660 – 664.
- [15] Y.H. Han, I.H. Choi, H.K. Kang, J.Y. Park, K.T. Kim, H.J. Shin, S. Moon, “Fabrication of Vanadium Oxide Thin Films with High-temperature Coefficient of Resistance using V₂O₅ / V / V₂O₅ Multi-layers for Uncooled Microbolometers”, *Elsevier, Thin Solid Films* 425 (2003) 260 – 264.

- [16] H. Miyazaki, I. Yasui, "Effect of Buffer Layer on VO_x Film Fabrication by Reactive RF Sputtering", Elsevier, Applied Surface Science (2005).
- [17] H.K. Kim, T.Y. Seong, Y.S. Yoon, "Effect of Platinum Co-Sputtering on Characteristics of Amorphous Vanadium Oxide Films", Elsevier, Journal of Power Sources 112 (2002) 67 – 75.
- [18] L.Z. Shuan, W.S. Tao, L.I. Jing, G.D. Hui, X.F. Chun, "Vanadium Oxide Thin Films Prepared by R.F. Magnetron Sputtering Method", Proc. SPIE Vol 5774 (2004) 148 – 151.
- [19] C. Chen, X. Yi, X. Zhao, B. Xiong, "Characterization of VO₂-based Uncooled Microbolometer Linear Array", Elsevier, Sensors and Actuators A 90 (2001) 212 – 214.
- [20] C. Petit, J.M. Frigerio, M. Goldmann, "Hysteresis of the Metal-Insulator Transition of VO₂; Evidence of the Influence of Microscopic Texturation", Journal of Physics Condensed Matter 11 (1999) 3259 – 3264.
- [21] Y.S. Yoon, J.S. Kim, S.H. Choi, "Structural and Electrochemical Properties of Vanadium Oxide Thin Films Grown by D.C. and R.F. Reactive Sputtering at Room Temperature", Elsevier, Thin Solid Films 460 (2004) 41 – 47.
- [22] H. Wang, X. Yi, S. Chen, "Low Temperature Fabrication of Vanadium Oxide Films for Uncooled Bolometric Detectors", Elsevier, Infrared Physics & Technology 47 (2006) 273 – 277.
- [23] F. Gracia, F. Yubero, J.P. Espinos, A.R. Gonzalez-Eliphe, "First Nucleation Steps of Vanadium Oxide Thin Films Studies by XPS inelastic peak shape analysis", Applied Surface Science 252 (2005) 189 – 195.

- [24] D. Zintu, G. Tosone, and A. Mercuri, "Dual ion beam sputtering vanadium dioxide microbolometers by surface micromachining," *Infrared Physics & Technology*, **43**, 245-250, 2002.
- [25] G.J Fang, Z. L. Liu, Y. Wang, Y.H. Liu, K.L. Yao, "Synthesis and Structural, Electrochromic Characterization of Pulsed Laser Deposited Vanadium Oxide Thin Films", *Amer. Vac. Society Journal Vac. Sci. Technol. A* 19(3) (2001) 887 – 892.
- [26] R.T.R. Kumar, B. Karunagaran, D. Mangalaraj, S.K. Narayandass, P. Manorari, M. Josep, V. Gopal, "Room Temperature IR Detection Using Pulsed Laser Deposited Vanadium Oxide Bolometer", *Proc. SPIE Vol. 5062* (2003) 425 – 432.
- [27] K.L. Van, H. Groult, A. Mantoux, L. Perrigaud, F. Lantelme, R. Lindstrom, R.B. Hadjean, S. Zana, D. Lincot, "Amorphous Vanadium Oxide Films Synthesised by ALCVD for Lithium Rechargeable Batteries", *Journal of Power Sources, Elsevier Vol. 7796* (2006).
- [28] A. Razavi, T. Hughes, J. Antinovitch, J. Hoffman, "Temperature Effects on Structure and Optical Properties of RF Sputtered VO₂", *American Vacuum Society Journal Vac. Sci. Technol. A* 7(3) (1989) 1310 – 1313.
- [29] A. Rogalski, "Infrared Detectors: Status and Trends", *Pergamon, Progress in Quantum Electronics* 27 (2003) 59 – 210.
- [30] F.Y. Gan, P. Laou, "Optical and Electrical Properties of Sputtered Vanadium Oxide Films", *Amer. Vac. Society Journal Vac. Sci. Technol. A* 22(3) (2004) 879 – 882.
- [31] K. Narumi, S. Yamamoto, A. Miyashita, Y. Aoki, H. Naramoto, "Formation of Vanadium Oxide by Ion Implantation and Heat Treatment", *IEEE* (1999) 990 - 993.

- [32] N. Alov, D. Kutsko, I. Spirovova, Z. Bastl, "XPS Study of Vanadium Surface Oxidation by Oxygen Ion Bombardment", Elsevier, Surface Science 600 (2006) 1628 – 1631.
- [33] N.C. Anh, H.J. Shin, K.T. Kim, Y.H. Han, S. Moon, "Characterization of Uncooled Bolometer with Vanadium Tungsten Oxide Infrared Active Layer", Elsevier, Sensors and Actuators A 123 – 124 (2005) 87 – 91.
- [34] R.T.R. Kumar, B. Karunagaran, D. Mangalaraj, S.K. Narayandass, P. Manoravi, M. Joseph, V. Gopal, R.K. Madaria, J.P. Singh, "Room Temperature Deposited Vanadium Oxide Thin Films For Uncooled Infrared Detectors", Pergamon, Materials Research Bulletin 38 (2003) 1235 – 1240.
- [35] S. Chen, H. Ma, S. Wang, N. Shen, J. Xiao, H. Zhou, X. Zhao, Y. Li, X. Yi, "Vanadium Oxide Thin Films Deposited on Silicon Dioxide Buffer Layers by magnetron Sputtering", Elsevier, Thin Solid Films 497 (2006) 267 – 269.
- [36] S.B. Wang, S.B. Zhou, G. Huang, X.J. Yi, "VO_x Thin Films Obtained by Ion Beam Sputtering and Oxidation Process", Elsevier, Surface & Coatings Technology 191 (2005) 330 – 334.
- [37] S.D. Hansen, C.R. Aita, "Low Temperature Reactive Sputter Deposition of Vanadium Oxide", Amer. Vac. Society Journal Vac. Sci. Technol. A 3 (3) (1985) 660 – 663.
- [38] T.J. Hanlon, R.E. Walker, J.A. Coath, M.A. Richardson, "Comparison Between Vanadium Dioxide Coatings on Glass Produced by Sputtering, Alkoxide and Aqueous Sol – Gel Methods", Elsevier, Thin Solid Films 405 (2002) 234 – 237.
- [39] Y.J. Park, K.S. Ryu, N.G. Park, Y.S. Hong, S.H. Chang, "RF Sputtered Vanadium Oxide Films", Journal of the Electrochemical Society 149(5) (2002) A597 – A602.

- [40] R.T.R. Kumar, B. Karunakaran, D. Mangalaraj, S.K. Narayandass, P. Manoravi, M. Joseph, V. Gopal, "Pulsed Laser Deposited Vanadium Oxide Thin Films For Uncooled Infrared Detectors", Elsevier, Sensors and Actuators A 107 (2003) 62 – 67.
- [41] P. Jin, K. Yoshimura, and S. Tanemura, "Dependence of microstructure and thermo-chronism on substrate temperature for sputter-deposited VO₂ epitaxial films," Journal of Vacuum Science and Technology A, **15**, 1113-1117, 1997.
- [42] S.H. Lee, H.M. Cheong, M.J. Seong, P. Liu, C.E. Tracy, A. Mascarenhas, J.R. Pitts, S.K. Deb, " Raman Spectroscopic Studies of Amorphous Vanadium Oxide Thin Films", Elsevier, Solid State Ionics 165 (2003) 111 – 116.
- [43] G.B. Stefanovich, A.L. Pergament, A.A. Velichko, L.A. Stefanovich, "Anodic Oxidation of Vanadium and Properties of Vanadium Oxide Films", Journal of Physics Condensed Matter 16 (2004) 4013 – 4024.